CAPE BRETON UNIVERSITY

Diversion of Crab Bodies from Landfill – Generation of High Value Biochar

By

Haley Elizabeth Armstrong

A thesis submitted in partial fulfillment of the requirements for the degree of

Bachelor of Science Honours (Chemistry)

Cape Breton University

Approved by

_____

Stephanie MacQuarrie, PhD, Department of Chemistry, Cape Breton University

_____

Martin Mkandawire, PhD, Department of Chemistry, Cape Breton University

_____

Karen Foss, BSc, Department of Chemistry, Cape Breton University

Date: _____

Abstract

Every year Louisbourg Seafoods Ltd. sends approximately 1000 tons of crab waste to landfills. Transport of this waste material is not only costly for them, but it is also burning a significant amount of fossil fuels. Louisbourg Seafoods Ltd. is currently investing in efforts to identify an environmentally beneficial disposal method for the considerable amount waste generated by processing of snow crab. For every crab processed one third of each crab body will end up in Canadian landfills. A proposed method for this waste stream is to generate biochar.

Crab based biochar was generated by slow pyrolysis at 400°C for 4 hours. The generated biochar was fully characterized by FT-IR, BET, XRD, TEM, and GC-MS. The crab biochar was found to have a surface area of 16.3 m^2/g by BET analysis. FT-IR and XRD showed there was a significant amount of calcium carbonate in the crab biochar. XRD showed the crystal structure is calcite.

A Palladium-Zinc-$CaCO_3$ catalyst was generated to catalyze the hydrogenation of alkynes to alkenes. This catalyst is hypothesized to be stereospecific for the cis-alkene product. The performance of the catalyst was analyzed by a simple hydrogenation of 2-butyne-1,4-diol. The Pd-Zn-$CaCO_3$ catalyst was active, however the product produced was butane-1,4-diol instead of cis-2-butene-1,4-diol. This means the catalyst is not stereospecific in its current state.

Table of Contents

List of Figures

List of Schemes

List of Tables

List of Terminology

$CaCO_3$	Calcium carbonate
CaO	Calcium oxide
CRB	Crab biochar
FCB	Forestry/crab biochar mixture
FOB	Forestry biochar
FT-IR	Fourier transform infrared spectroscopy
GC-MS	Gas chromatography mass spectroscopy
Pd	Palladium
TEM	Transmission electron microscope
XRD	X-ray powder diffraction
Zn	Zinc

Acknowledgments

I would like to thank Dr. Stephanie MacQuarrie for being the best supervisor anyone could ever have. Without her constant support I do not believe I would have been able to finish this thesis. I am so fortunate to be able work with and learn from such a positive role model. I would also like to thank my committee, Karen Foss and Dr. Martin Mkandawire, for their constant input and guidance over the past year.

I would like to thank Judy MacInnis for all her help and support over the past year. She was always willing to help even with the smallest question. I would also like to thank Dr. Trisha Ang and Dr. Andrew Carrier for their help and input with my hydrogenation reaction. In addition I would like to thank everyone at MUN who helped with running elemental analysis and the yields of the biochar production.

I would like to thank everyone in the MacQuarrie group, for their help and for dealing with the "interesting" smells in the lab when dehydrating the crab bodies. I would especially like to thank Dr. Shanghuan Feng for all of his involvement. I would also like to than Adam Mugridge and Louisbourg Seafoods Ltd. for providing the crab bodies. I would like to thank Divert Nova Scotia for providing funding to support my project.

I would also like to acknowledge my fellow honours students: Vincent Andrea, Jennifer MacDonald, and Christopher MacKenzie. It was extremely comforting to have people going through the same challenges as myself. I am very grateful to be able to have conversation with them and to be able to overcome these challenges together.

Lastly, I would like to thank my friends and family for keeping me sane during my academic career. I do not know where I would be without all of their constant love and support.

1 Introduction

1.1 Background

Snow Crab (*Chionoecetes opilio*) fisheries are a vital resource for Atlantic Canada. The fishery has been declared the second most important fishery by The Department of Fisheries and Oceans.[1] Snow crab are a species of spider crab that inhabits the cold frigid waters of Northwestern Atlantic and Northern Pacific oceans. In Atlantic Canada snow crab is harvested off the coast of Cape Breton Island, and off the coast of Newfoundland and Labrador.[2] In 2016 Canadian fisheries harvested 48,000 metric tons of snow crab.[3] During the processing of snow crab, only the crab legs are retained for their meat, with the rest of the crab bodies (approximately 1/3 of the crab) considered waste, and often sent to landfills.[1] Louisbourg Seafoods Ltd. is currently investing in efforts to identify an environmentally beneficial disposal method for the considerable amount of crab waste generated.

Crab shells are composed of chitin (15-40%), proteins (20-40%), and calcium carbonate (20-50%).[4,5] Chitin is one of the most abundant and valuable biomaterials on earth.[6] It is found in the external shells of crustaceans, and in the beaks and cuttlebones of cephalopods. Chitin is chemically known as β-(1,4)-N-acetyl-D-glucosamine.[7] The processing of chitin is limited by the insolubility of chitin in many solvents. However, strong acid can be used to extract chitin from crustacean shells, followed by alkali treatment to remove the proteins, minerals, and lipids, this extraction method does not make economic sense when the starting biomass is the wasted crab bodies. The excessive generation of acidic and also alkaline wastewater to retain a low percent of chitin, and it is not viable.[5,8] Since the $CaCO_3$ makes up the largest percentage of matter in the crab shell, it makes more sense to find a route to extract or take advantage of that high value material. $CaCO_3$ is an

abundant biomineral and has three crystalline polymorphic forms calcite, aragonite, and vaterite.[9–12] Calcite is the most plentiful of the three polymorphs because it is somewhat more stable than aragonite. However, both from are common in nature. Vaterite is metastable and is very rare in nature. Current information suggests that calcium carbonate exists in an amorphous form but is very rare.[12] Various organisms use $CaCO_3$ as a component in their skeletons or in protective shells, and it is used at the visual device in the brittle star.[9] $CaCO_3$ is also used as a building material by engineers.[12] By finding a way to access the $CaCO_3$ in the crab bodies and converting the rest of the organics to biochar, several potential applications for this waste material are recognized. By exploring these applications, we can begin to eliminate crab waste from our landfills.

1.2 Biochar production and applications

Biochar production diverts carbon into a more stable form that decomposes at a much slower rate when compared to its parent biomass.[13] Biochar is produced through pyrolysis, the process of burning biomass between 350-700°C, and under low oxygen conditions.[6,14,15] Pyrolysis of biomass has three major products: bio-oil (pyrolytic oil), syngas (synthesis gas), and biochar.[6] Biochar is amorphous, has a high pore volume, and can be rich in surface functional groups.[4,16] Most biochar is currently generated from lignocellulose biomass with very few examples of biochar from crustacean waste. Biochar that has been generated from crab waste is rich in calcium. The calcium can then be utilized in several different situations, from environmental cleanup to being used as a catalyst.

Dai, et al. showed that biochars that are high in calcium, magnesium, iron, or aluminum, could also be used to remove/recover phosphorous from water. Phosphorous is a

finite resource, and if excess amounts are introduced to aquatic environment, can cause eutrophication. Removal/recovery of phosphorous from aquatic environments can help to control eutrophication, and also replenish the phosphorous resources.[4] Following adsorption of phosphorous, the biochar can be used as a slow releasing fertilizer.[17] Biochar made from crab bodies is particularly good for phosphorous removal because of the high content of calcium in the bodies in the form of $CaCO_3$, which is a particularly good adsorbent of phosphate.[4] Therefore, no additional treatment of the biochar derived from crab waste is necessary for it to be effective in phosphorous removal and recovery.

Xiao, et al. developed biochar from crayfish shells (another crustacean), for sorption of heavy metals. Biochar was developed at different temperatures to determine the optimum temperature to improve the capacity of the biochar to Pb(II). In addition, the effects of pH, ionic strength, and the presences of competitive ions on the sorption of Pb(II) were also investigated. They concluded that the sorption of Pb(II) onto crayfish biochar was dependent on temperature, pH and ionic strength. Crayfish biochar generated at 600°C showed the highest sorption capacity, 190.7 mg/g.[6] Similar studies have been done with biochar generated from lignocellulose biomass.[18] Mohan, et al. developed biochar from pine wood, pine bark, oak wood, and oak bark. The oak bark biochar showed the highest sorption capacity for Pb(II) of the four biochars at 13.10 mg/g. The next best was pine wood biochar, 4.13 mg/g, followed by pine bark, 3.00 mg/g, and lastly oak wood, 2.62 mg/g.[18] Mohan, et al. attributed the higher sorption capacity of the oak bark biochar to the higher surface area, larger pore volume, and higher calcium content of the char.

Magnacca, et al. used chitin derived from snow crab to make biochar for possible environmental and electrochemical applications. The biochar was generated at mild pyrolysis

conditions, between 290-540°C. Two applications of the chitin biochar were investigated. One application was to determine the absorbance capacity and selectivity towards CO_2. The experimental results showed that the chitin-based biochar generated at 440°C is able to selectively and reversibly interact with CO_2 and is potentially useable for environmental applications.[7] The addition of nitrogen groups to the surface of the forestry biochar can increase capacity for CO_2 adsorption.[19–21] Zhang, et al. showed that biochar generated from forestry residue prepared at 800°C with enhanced nitrogen was capable of adsorbing 2.25 mmol/g of CO_2, compared to untreated biochar adsorbing 0.89 mmol/g of CO_2.[21] The chemical composition of the biochar derived from chitin and much more complex proteins of crab bodies will be enhanced (i.e. Nitrogen from amino acids, proteins, and chitin will enhance the overall N concentration in the resulting biochar). The second application Magnacca, et al. investigated was to test the chitin-based biochar as a possible cathode in lithium-sulfur batteries. When biochar that is produced at 294°C is being used as cathode material shows high polarization and stable discharge capacity. Alternatively, the biochar generated at 440°C and 540°C shows low polarization and higher stable discharge capacities when being used a cathode. The biochar generated at higher temperatures also shows high coulombic efficiencies.[7]

Calcium also plays a large role in catalysis. For example calcium catalyst can be used in transesterfication reactions, biodiesel production, and hydrogenation reactions[22–25]. Boey, et al. used mud crab shells as a source of calcium to make a catalyst for the transesterfication of palm oil to make biodiesel. The crab bodies were dried and then heated at 700°C to transform any $CaCO_3$ into calcium oxide. The calcium oxide was then used as the catalyst for biodiesel production.[22] Suppes, et al. used $CaCO_3$ as a catalyst for alcholysis reactions.

$CaCO_3$ was successfully used to catalyze the reaction between soybean oil and ethylene glycol.[23] In 1952, Lindlar developed a catalyst for selective hydrogenation of unsaturated carbon-carbon bonds (alkynes to cis-alkenes).[26] The catalyst consists of palladium supported on $CaCO_3$, and poisoned with lead.[25,26] Other metals, like zinc, have been used in place of lead for the poisoning of the catalyst.[24] Chaudhari, et al. used the Pd-Zn-$CaCO_3$ catalyst to hydrogenate butynediol to cis-butenediol (Scheme 1). Due to the $CaCO_3$ content of the crab biochar, it has potential to be used as the $CaCO_3$ support to generate a catalyst similar to Lindlar's catalyst. Which leads us to the point of this thesis to examine whether crab biochar can be used as a heterogeneous catalyst.

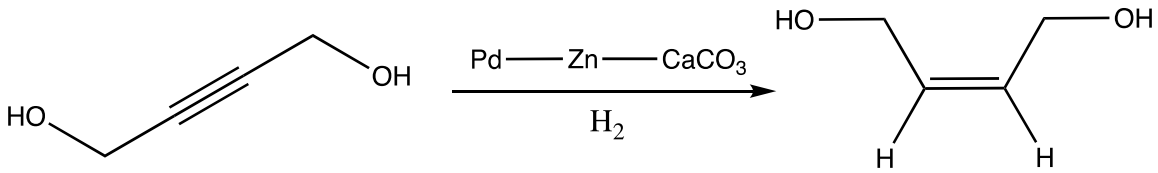

Scheme 1 Hydrogenation of 2-butyne-1,4-diol to cis-2-butene-1,4-diol catalyzed by Pd-Zn-$CaCO_3$.

1.3 Research Objectives

The objectives of this research are as follows: generate biochar from snow crab body waste, determine the impact of heterogeneity of the starting biomass on biochar and fully characterize each biochar produced (surface area, pH, surface functionalization). This research will also attempt to exploit the $CaCO_3$ content in the crab biochar to generate a cheap, greener alternative heterogeneous catalyst, in particular a palladium-zinc-$CaCO_3$ catalyst.

2 Experimental/Methods

2.1 Materials and equipment

All chemicals used in the experiments were reagent grade chemicals. Crab bodies were supplied from Louisbourg Seafoods. Infrared analysis was performed on a Thermo Nicolet 6700 FT-IR Spectrometer (64 scans, 4cm resolution). A Bruker D8 diffractometer with Cu Kα radiation was used to obtain Powder XRD patterns. BET analysis was obtained using a Micromeritics ASAP 2020 Surface Area and Porosity Analyzer. TEM images were obtained using a Hitachi HT7700 Transmission Electron Microscope. An Agilent 5890 GC with 5973 MSD was used to obtain a GC-MS spectrum. Distilled water was collected from Milipore Elix ® Essential 15 UV system.

2.2 Biochar Production

2.2.1 Crab Biochar

Crab bodies were obtained from Louisbourg Seafoods Ltd. Crab bodies were dried at 100°C for 24 hours to reduce the water content. The dried crab bodies are pyrolyzed at 400°C for 4 hours.

2.2.2 Crab and Forestry Biochar Mix

A 50% crab body, 50% forestry waste (birch trees) biochar was generated by first drying each feedstock in an oven at 100°C for 24 hours to remove any moisture. A 1:1 mixture (by weight) of dried crab bodies and dried forestry waste was measured out before pyrolysis. Pyrolysis occurred at 400°C for 4 hours. The yield for slow pyrolysis was 55% biochar, and 20% bio-oil. The yield for fast pyrolysis was 52% biochar and 31% bio-oil.

2.3 $CaCO_3$ Removal

To remove $CaCO_3$, CRB (100 mg) was mixed with water (5 mL) in a round bottom flask. This was repeated to make three round bottom flasks with biochar and water. To one of the flasks 37% hydrochloric acid (less than 1 mL) was added. This flask was stirred with a magnetic stirrer for 48 hours at room temperature. The second flask was stirred with a magnetic stirred for 48 hours at 80 °C. Flask 3 was stirred with a magnetic stirrer for 48 hours at room temperature.

2.4 Catalyst Production

This is based on the procedure by Lindlar & Dubuis and Chaudhari, R. V. et al. Palladium chloride (0.0167 g, 0.0942 mmol) is dissolved in concentrated hydrochloric acid (3.6 mL). Stirring and heating the solution to 30 °C is required to full dissolve all of the $PdCl_2$. The palladium chloride acid solution was diluted to approximately 100 mL with distilled water and added to a three-necked round bottom flask. The round bottom flask was then immersed in an 85°C water bath. CRB (1.00 g) was added carefully to the solution. It should be noted that the CRB was assumed to be 20% $CaCO_3$ for this experiment. This was based on the initial results from the $CaCO_3$ removal experiment. The $PdCl_2$ and $CaCO_3$ mixture was allowed to stir rapidly for 1 hour. Keeping the mixture at 85°C, 5% sodium formate (NaCOOH) solution (6.0 mL) was added to the mixture with vigorous stirring. After several minutes a further addition of 5% NaCOOH solution (4 mL) was added to the mixture and was allowed to stir for 1 hour. The Pd-$CaCO_3$ catalyst is then filtered and washed with 10 portions of water (20 mL).

The wet catalyst is then mixed with water (60 mL) and 20% zinc acetate ($ZnC_4H_6O_4$) solution (18 mL) and transferred to a round bottom flask. The mixture was heated under reflux for 30 minutes. The catalyst is then filtered and washed with 4 portions of water (20 mL) and the vacuum filtration apparatus was used to suck any remaining moisture off the catalyst. The catalyst was then dried in a 70°C oven for 24 hours.

2.5 Hydrogenation Reaction

A 10 mM solution of 2-butyne-1,4-diol in methanol (150 mL) and the crab biochar Pd-Zn-$CaCO_3$ catalyst (1.0 mol%) were charged into a three-necked round bottom flask. The contents of the flask were flushed with hydrogen. The reaction was started by turning on the stirrer. The reaction was stirred rapidly for approximately one hour. The reaction was then stopped and the Pd-Zn-$CaCO_3$ catalyst was removed by vacuum filtration. Both the catalyst and the filtrate were collected for further analysis.

3 Characterization

3.1 Characterization of Biochar

3.1.1 FT-IR

Fourier Transform Inferred spectra were collected using a Thermo Nicolet 6700 FT-IR Spectrometer. The computer software to process the data was Omnic. Sample preparation consisted of making potassium bromide pellet(s) with biochar as the analyte. IR spectra were obtained for the crab biochar (CRB), the crab/forestry biochar (CFB), and the forestry biochar FOB (Figure 1). The spectra were used to determine functionalization of the three biochars.

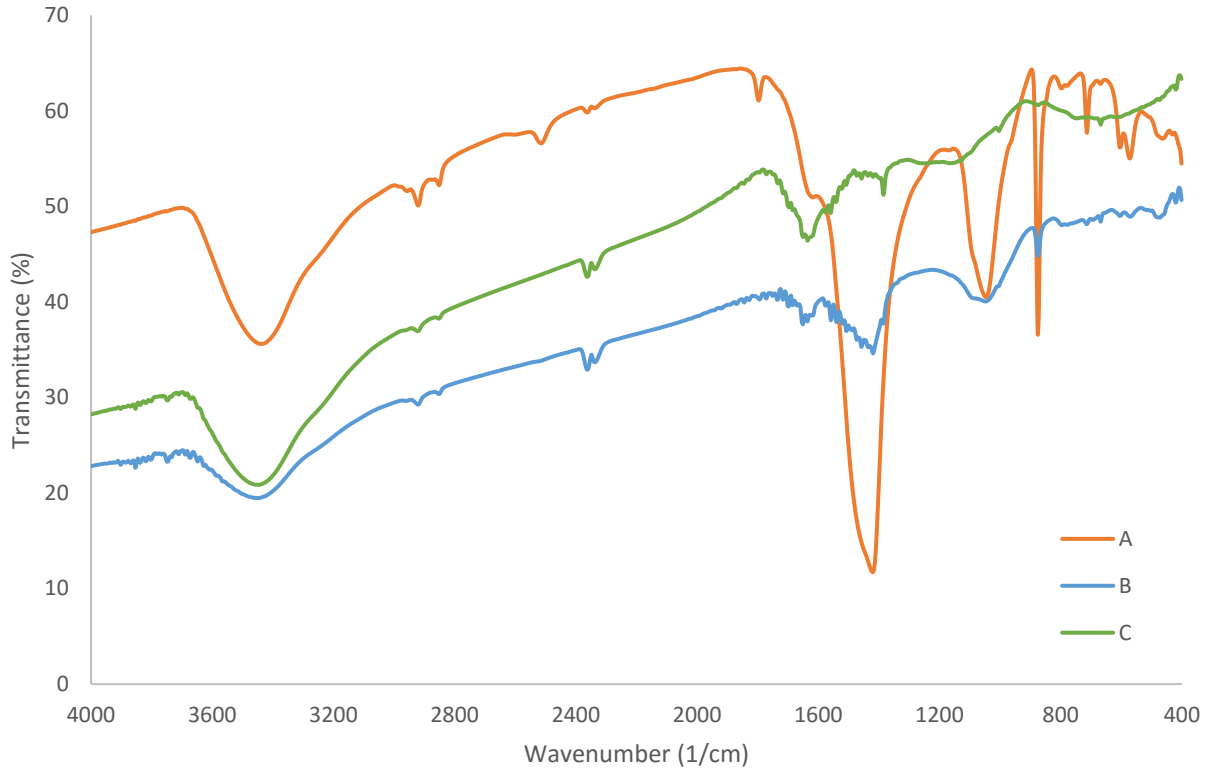

Figure 1 FT-IR spectra for CBR (orange), FCB(blue), and FOB (green).

The most prominent peaks in the CRB spectra (figure 1) are at 1420 cm^{-1}, 875 cm^{-1}, and 715 cm^{-1}. These bands are characteristic of $CaCO_3$.[4] There is a small peak at 1580 cm^{-1} that is characteristic for calcium oxide. The sharp bands at 875cm^{-1} and 715 cm^{-1} are characteristic of the rocking and bending vibrations for CO_2^{2-} as well as CaO[27]. These peaks are also present in the spectra for the CFB (figure 1). However, they are not as intense because the concentration of $CaCO_3$ and CaO in the FCB is significantly less than the concentration in CRB. There is also a peak around 1040 cm^{-1} in both the CRB and the CFB. This peak is likely due to C-C stretching. These peaks are not present in the spectra for forestry biochar (figure1).

FT-IR spectra was also obtained for pure CaO and $CaCO_3$ (figure 2). The peaks around 1420 cm^{-1}, 875 cm^{-1}, and 715 cm^{-1} are also present in the spectra for $CaCO_3$. And small peaks are present at 1580 cm^{-1}, !420 cm^{-1}, 875 cm^{-1} are present in the spectra for CaO. This is conclusive that the CRB and the CFB both contain $CaCO_3$ and CaO.

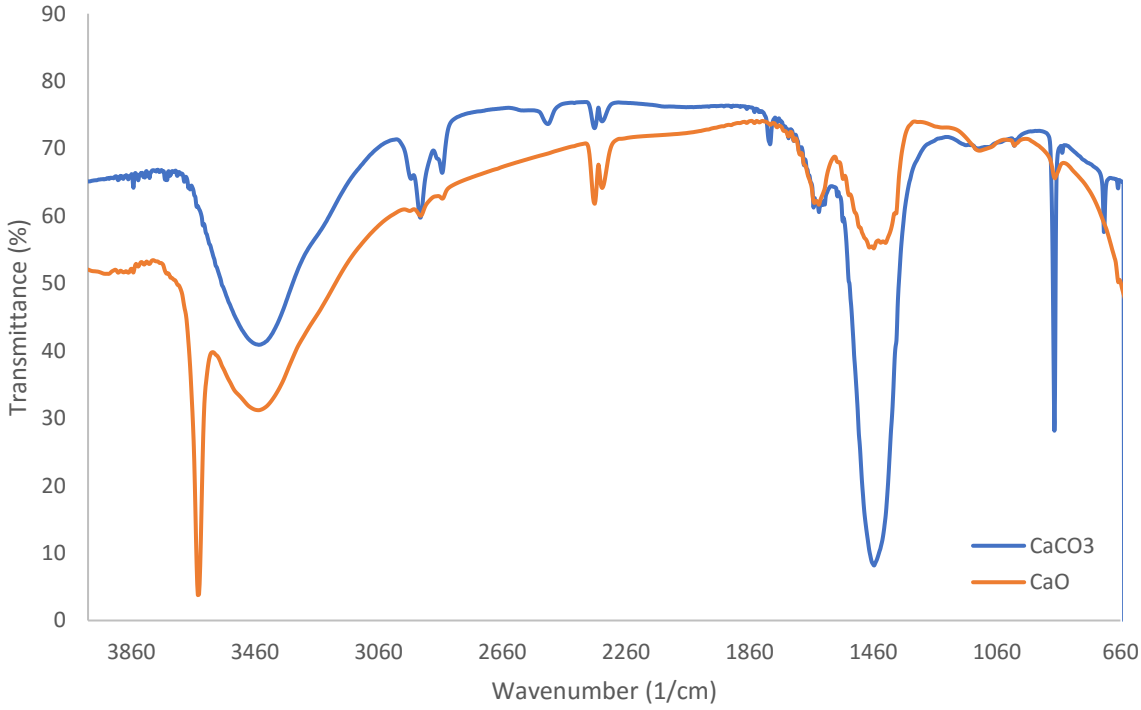

s

Figure 2 FT-IR for CaO (orange) and $CaCO_3$ (blue).

FT-IR was also obtained for the dried crab bodies (figure 3). The peaks around 1420 cm^{-1}, 875 cm^{-1}, and 715 cm^{-1} are also present in this spectrum. However, the peaks are significantly smaller. This indicates that during the generation of biochar, some quantity of organic fragments will be lost during pyrolysis. This causes the concentration of the calcium compounds to increase.

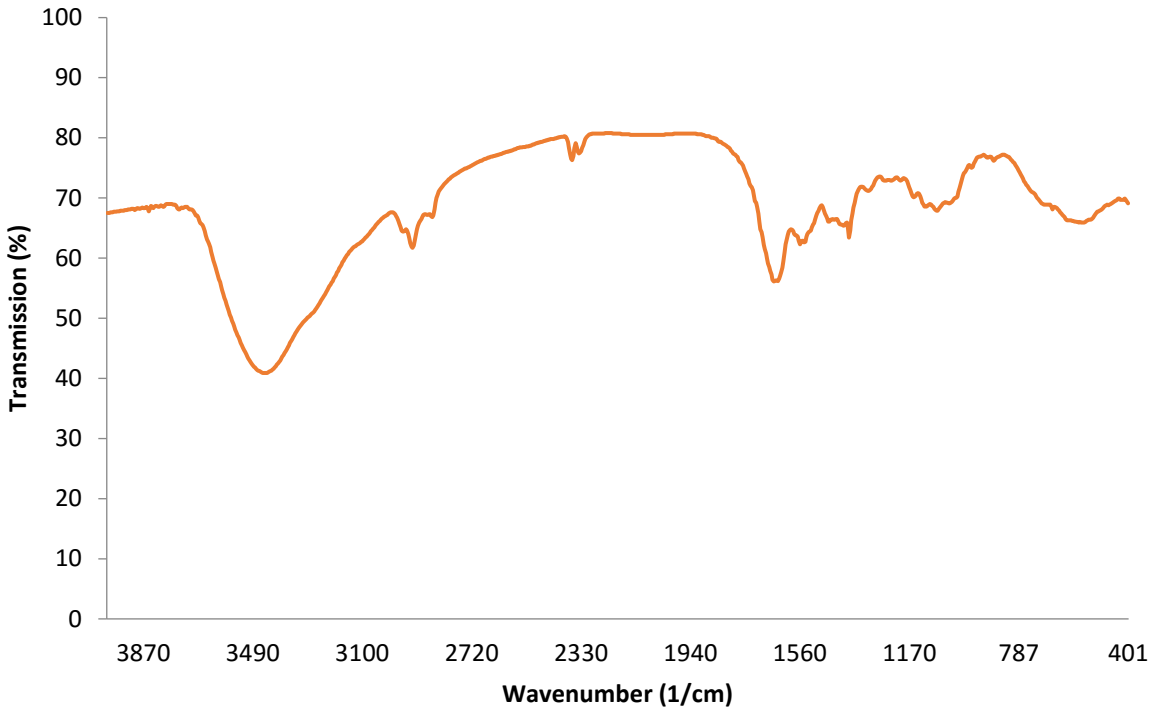

Figure 3 FT-IR for dehydrated crab bodies.

3.1.2 XRD

XRD was performed on a Bruker D8 diffractometer with Copper Kα radiation source. The software used to collect the data was Diffrac.commander and the software used to analyze the interference patterns was called Diffrac.EVA. Sample preparation consisted of grinding the sample into a very fine powder and placed in the sample holder. The sample was flattened as much as possible to make sure the x-rays would hit the sample evenly. Excess powder was removed from the sides of the sample holder to prevent interference. The parameters used for obtaining the diffractograms were scanned from 10-90° with a step size of 0.05° and a step time of 1 second.

From the XRD interference patterns for the CRB (figure 4) the crystal structure is for $CaCO_3$ is present. This is indicated by the peak at 29.4° and several smaller peaks in the

diffractogram[4]. This interference pattern is characteristic of the crystalline structure for calcite. This peak is also present in the CFB (figure 5).

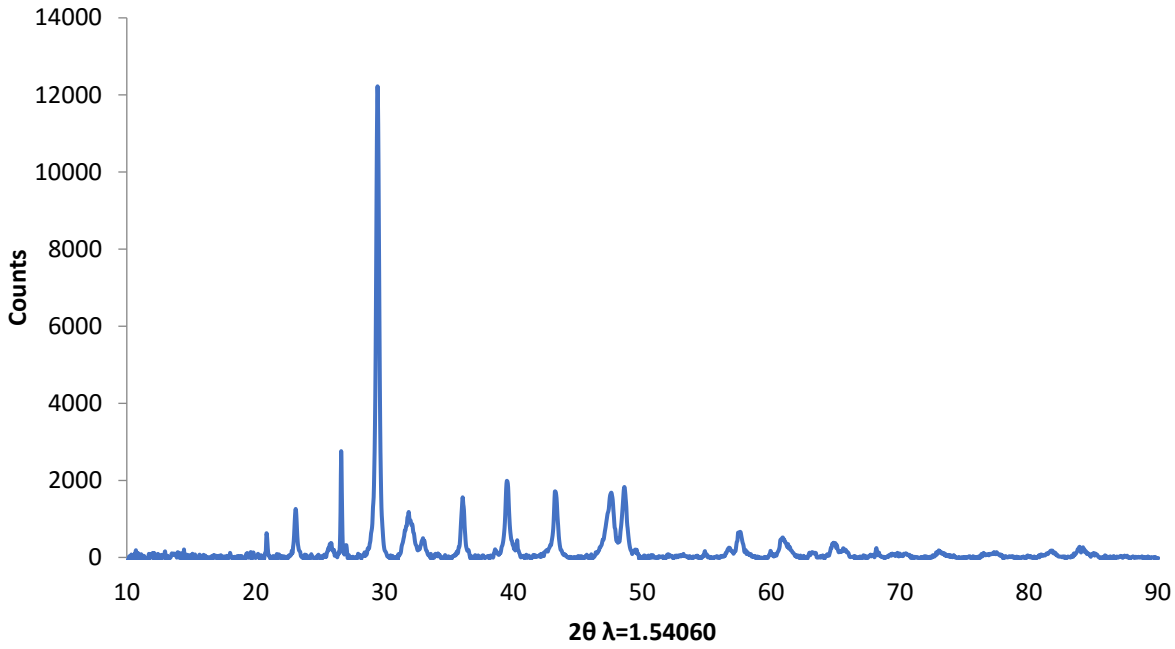

Figure 4 Diffractogram for CRB.

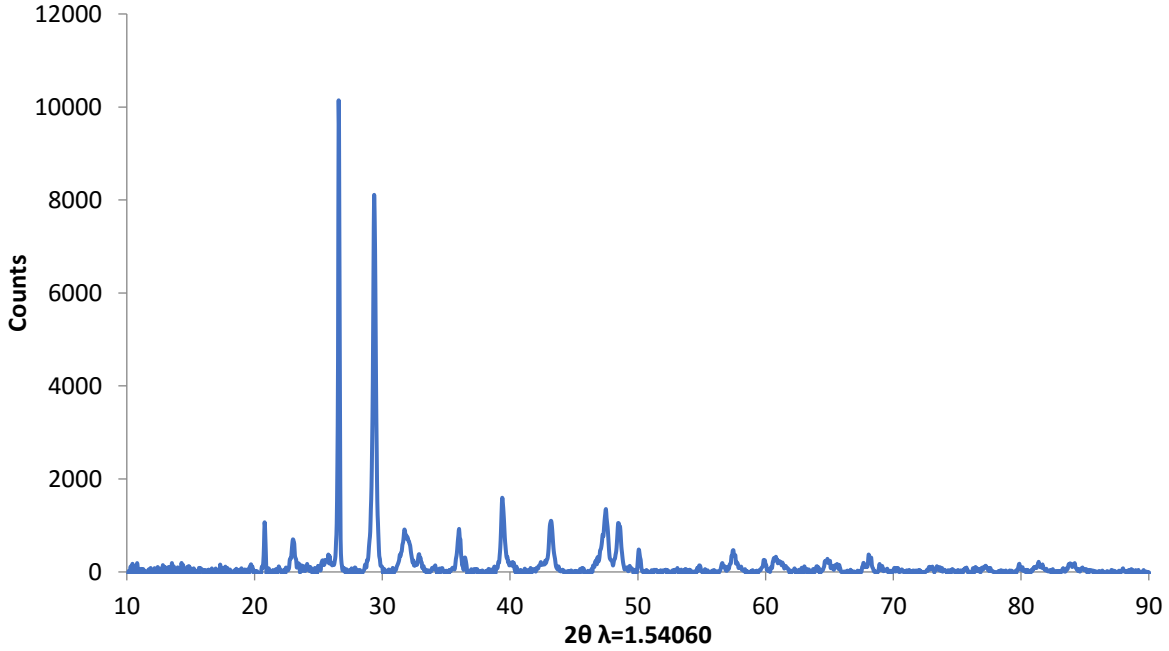

Figure 5 Diffreactogram for FCB.

There are no significant patterns seen in the FOB (figure 6). This was expected because there is no significant crystal structure in the FOB because the forestry waste does not have a crystal structure.

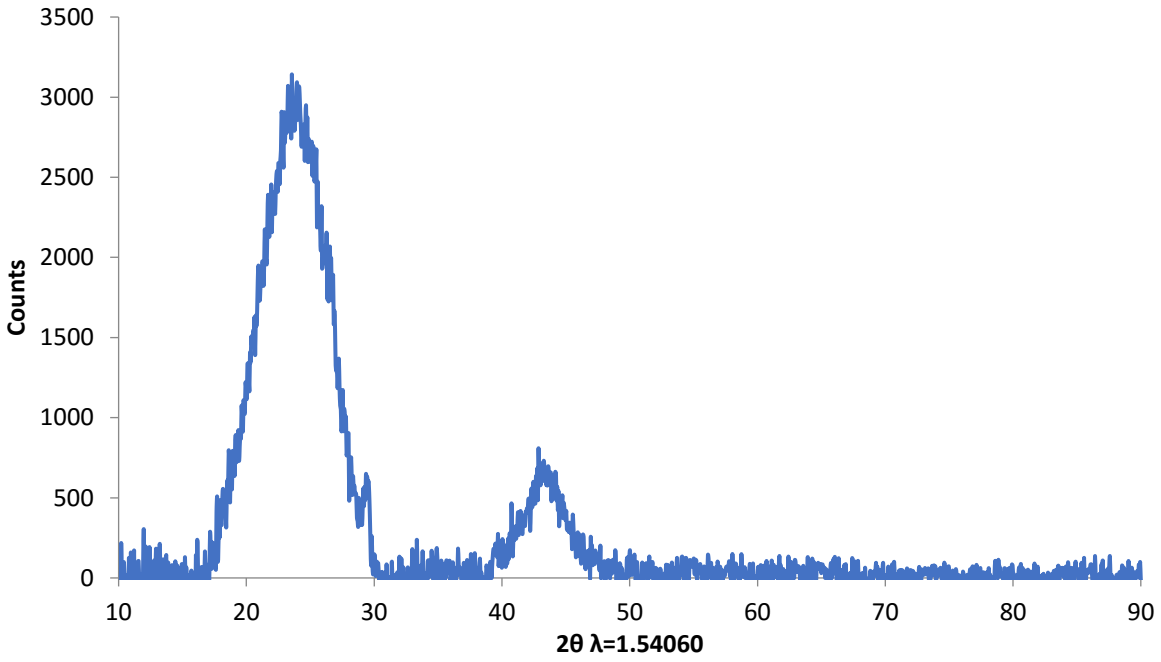

Figure 6 Diffractogram for FOB.

A diffractogram was also obtained for $CaCO_3$ (figure 7). The interference pattern is extremely similar to the diffractogram for crab biochar and the CFB. From a library search in the XRD software it shows this pattern is characteristic of calcite. Interference patterns for aragonite would have significant interference signals at 26°, 46°, and 48.5°. Interference patterns for vaterite would have significant interference signals at 25°, 33°, and 43.5°.[28]

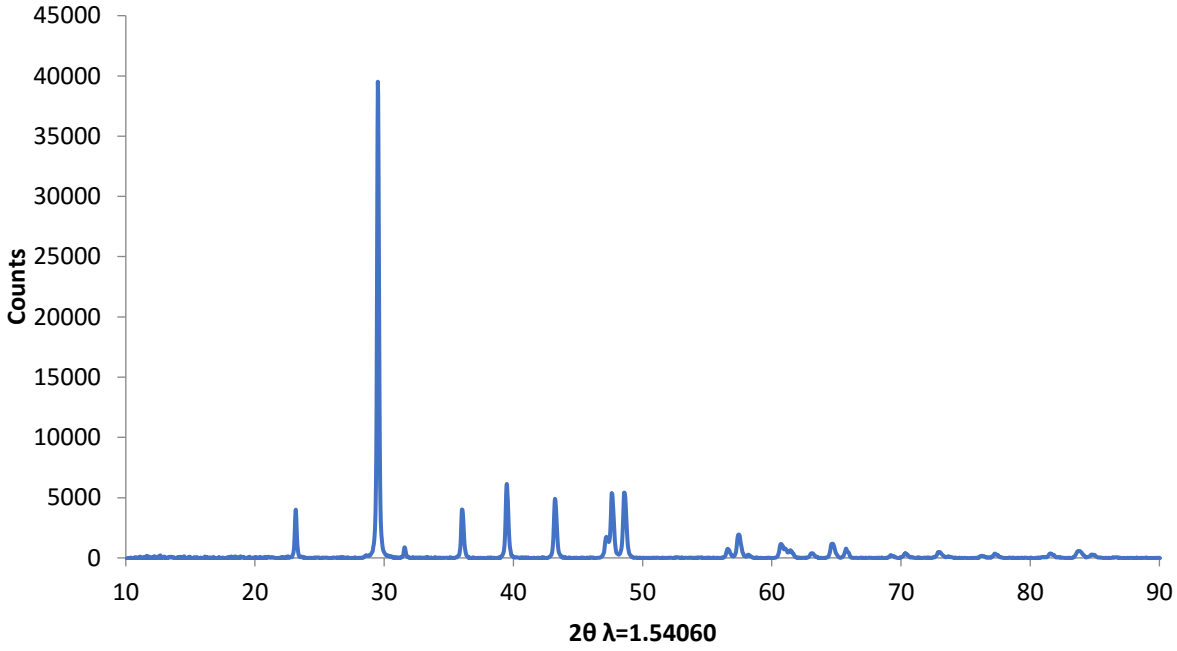

Figure 7 Diffractogram for $CaCO_3$.

3.1.3 Elemental Analysis

Elemental analysis was obtained using a Perkin Elmer 2400 series II CHNS analyzer. Due to the composition of crab bodies the only thing that can be concluded is there is nitrogen present in the crab biochar as well as in the crab/forestry mix biochar (Table 1). This nitrogen would most likely come from the proteins and chitin found in the bodies composition. The nitrogen content for the crab biochar is higher than the nitrogen content for the forestry/crab mix biochar. This is because of the forestry content in the FCB. There is nothing in the forestry waste to donate nitrogen content to the biochar.

Type of Biochar	C:H	C:N
Crab	100:(-1.35)	100:3.72
Forestry Crab Mix	100:1.56	100:2.49

Table 1 Hydrogen and nitrogen content for the CRB and FCB.

3.1.4 TEM

TEM images were obtained using a Hitachi HT7700 Transmission Electron Microscope equipped with a tungsten filament. Samples were prepared by dispersing a small amount of the biochar samples in ethanol. The samples were sonicated to obtain an evenly dispersed solution. Next 1 μL of the sample was pipetted onto a 200-mesh copper grid treated with formvar and carbon coating. The excess ethanol was blotted off the grid with a piece of filter paper.

From the TEM images it can be noted that the CRB has ordered particle arrangement (figure 8) as well as amorphous particle arrangement (figure 9). The ordered arrangement could be from the arrangement of chitin in the crab bodies. Similar structural arrangement is seen in TEM images for FCB (figure 10 and 11), and the dehydrated crab bodies (figure 12 and 13).

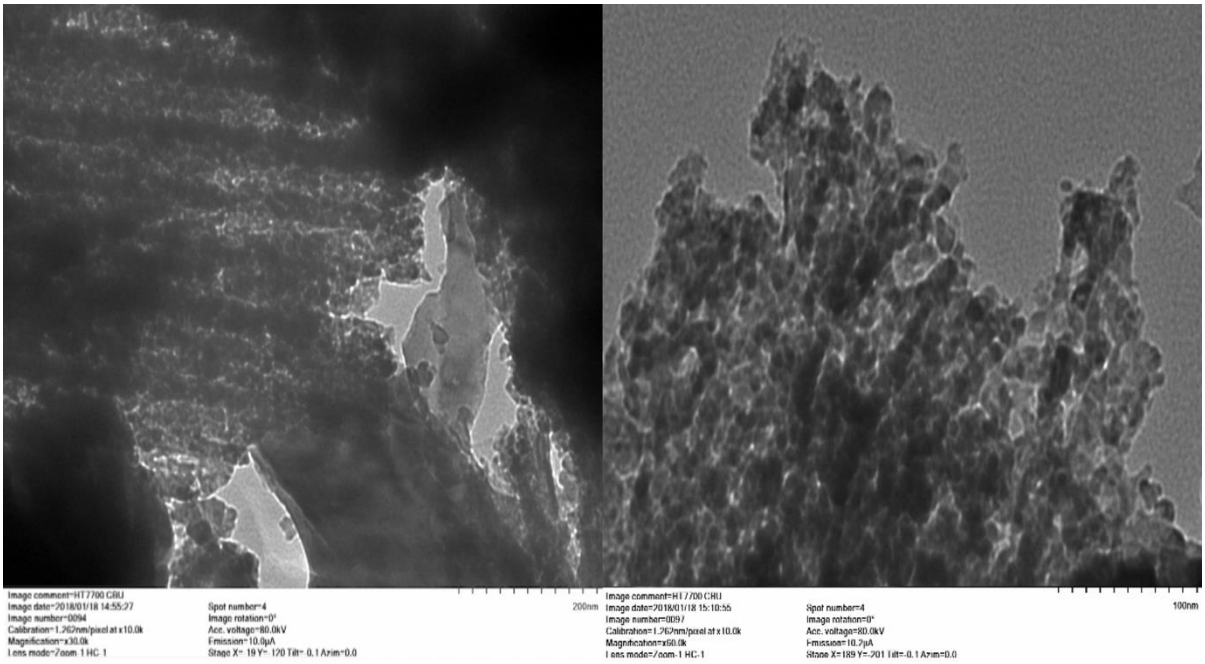

Figure 8 TEM images of CRB showing ordered particle arrangement (left) and an amorphous region (right).

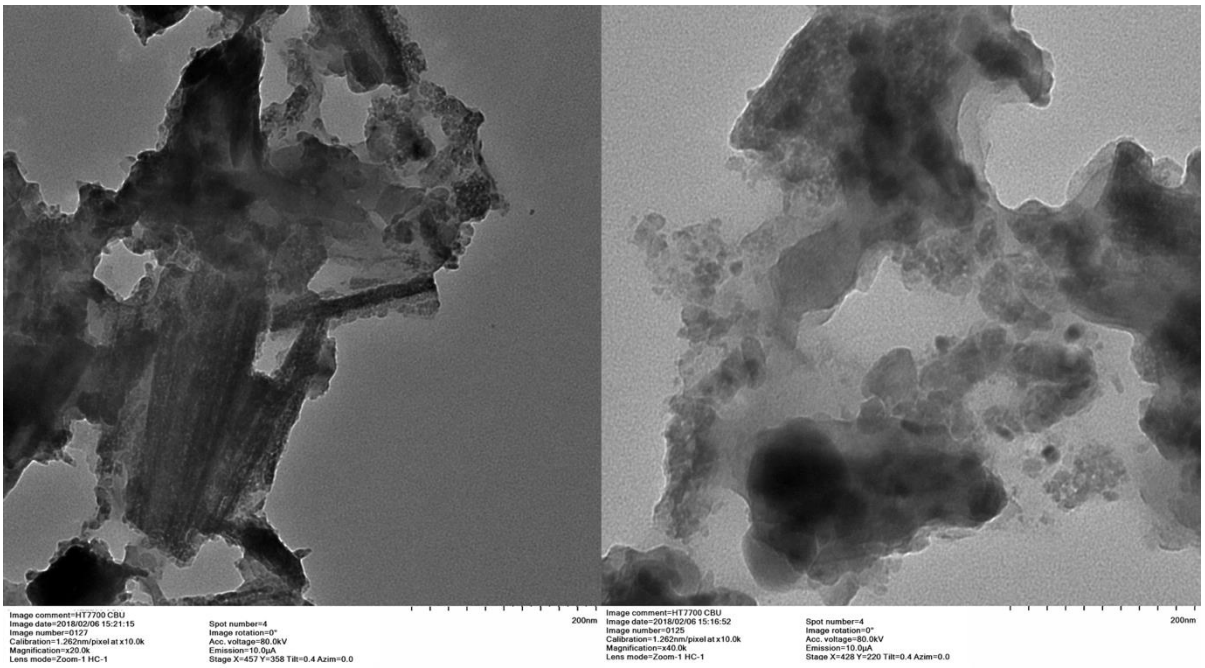

Figure 9 TEM image for FCB showing ordered particle arrangement (left) and an amorphous region (right).

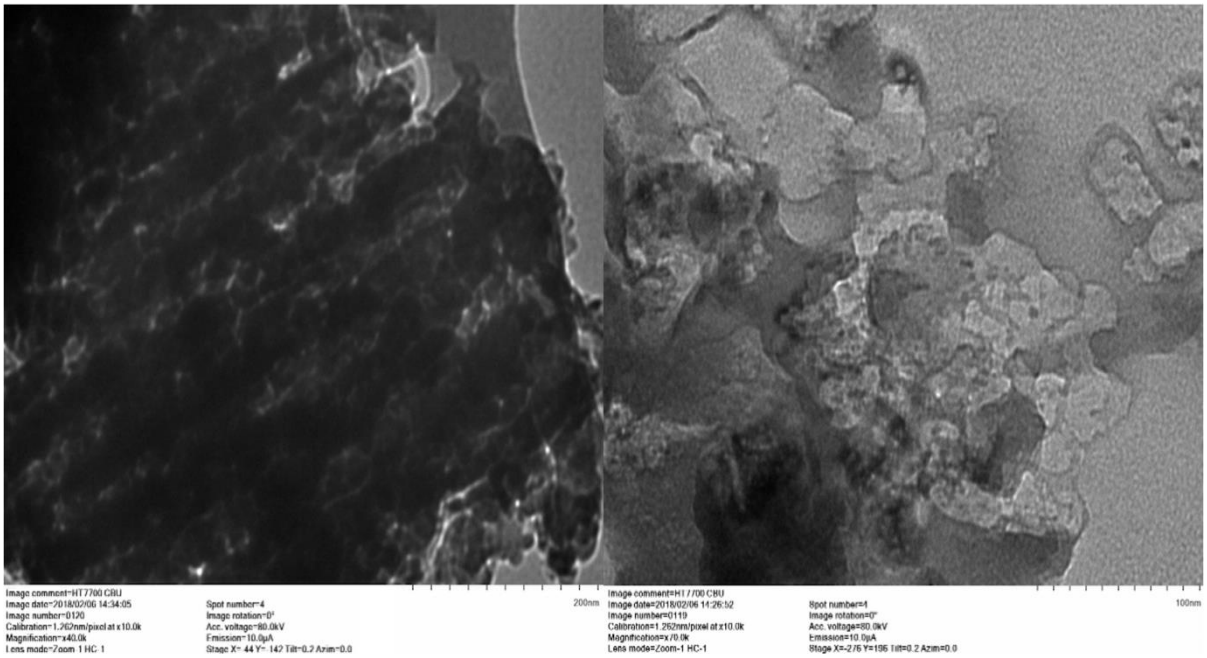

Figure 10 TEM image of dehydrated crab bodies showing ordered particle arrangement (left) and an amorphous region (right).

3.1.5 Physical Characteristic of Biochar

A Micromeritics ASAP 2020 Surface Area and Porosity Analyzer was used to determine the surface area for CRB, FCB, and FOB. The software used was ASAP 2020 V4.00. The surface area of the CRB, FCB, and FOB were found to be 16.3 m^2/g, 43.7 m^2/g, and 184 m^2/g respectively. The surface area for the FOB is almost twelve times larger than the surface area of the CRB. So CRB is not as porous or has smaller pores when compared to FOB. The surface area of FCB is larger than the CRB but smaller than FOB. This is likely due to the combination of the crab and forestry waste; most of the surface area is from the forestry waste.

The pH of each biochar was determined by mixing a small amount of biochar in small amount of water (about 1:10). The pH was measured using Hydrion Spectral pH Paper. The

pH for CRB, FCB, and FOB was found to be 11, 8, and 7 respectively. The increased pH of CRB is likely due to the $CaCO_3$ content.

3.2 Characterization of Biochar Catalyst

3.2.1 XRD

The interference pattern for the Pd-Zn-$CaCO_3$ catalyst was obtained using a Bruker D8 diffractometer with Copper Kα radiation source. When comparing the interference patterns for CRB and the Pd-Zn-$CaCO_3$ catalyst many of the interference signals are similar (figure 14). There are three peaks in the Pd-Zn-$CaCO_3$ catalyst diffractogram that indicate a presence of palladium. These interference signals are around 33.5°, 40.5°, and 47.6°.[29] This is an indication the palladium was successfully added onto CRB.

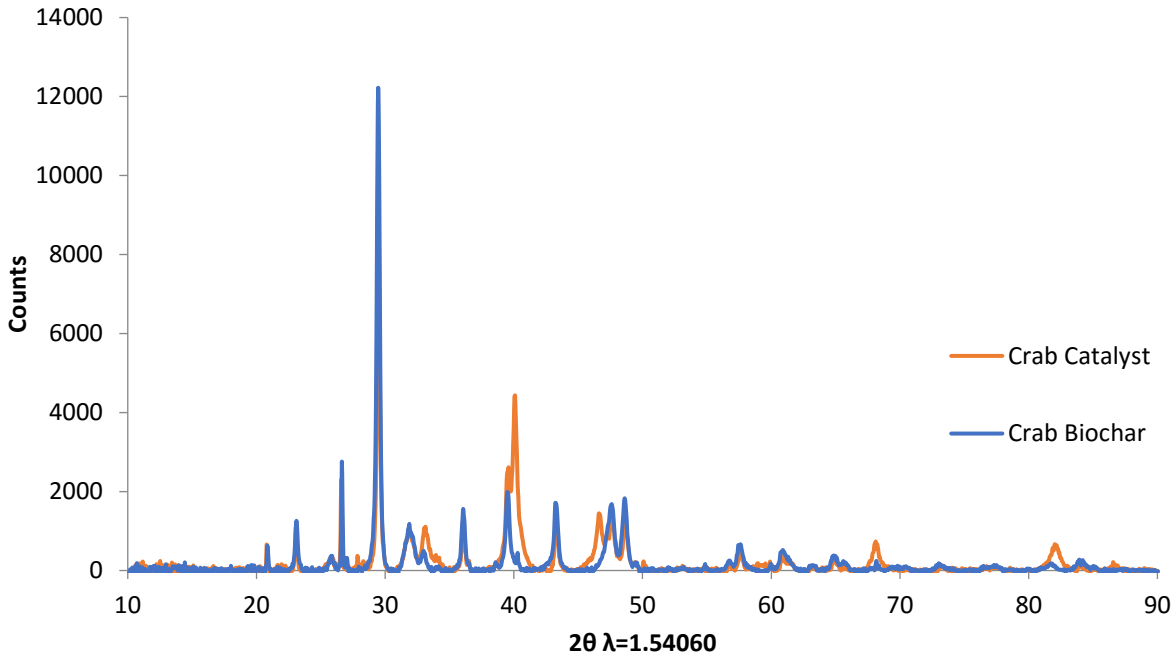

Figure 11 Diffractogram for CRB (red) and Pd-Zn-$CaCO_3$ catalyst (black).

3.2.2 TEM

TEM images were obtained using a Hitachi HT7700 Transmission Electron Microscope. Sample preparation was performed the same way as in section 3.1.4. The TEM images of the biochar catalyst do contain similar structures when compared to CRB, however there are small round particles on the catalyst (figure 15). This is likely the palladium and zinc that was added on the to the CaCO3 in the biochar.

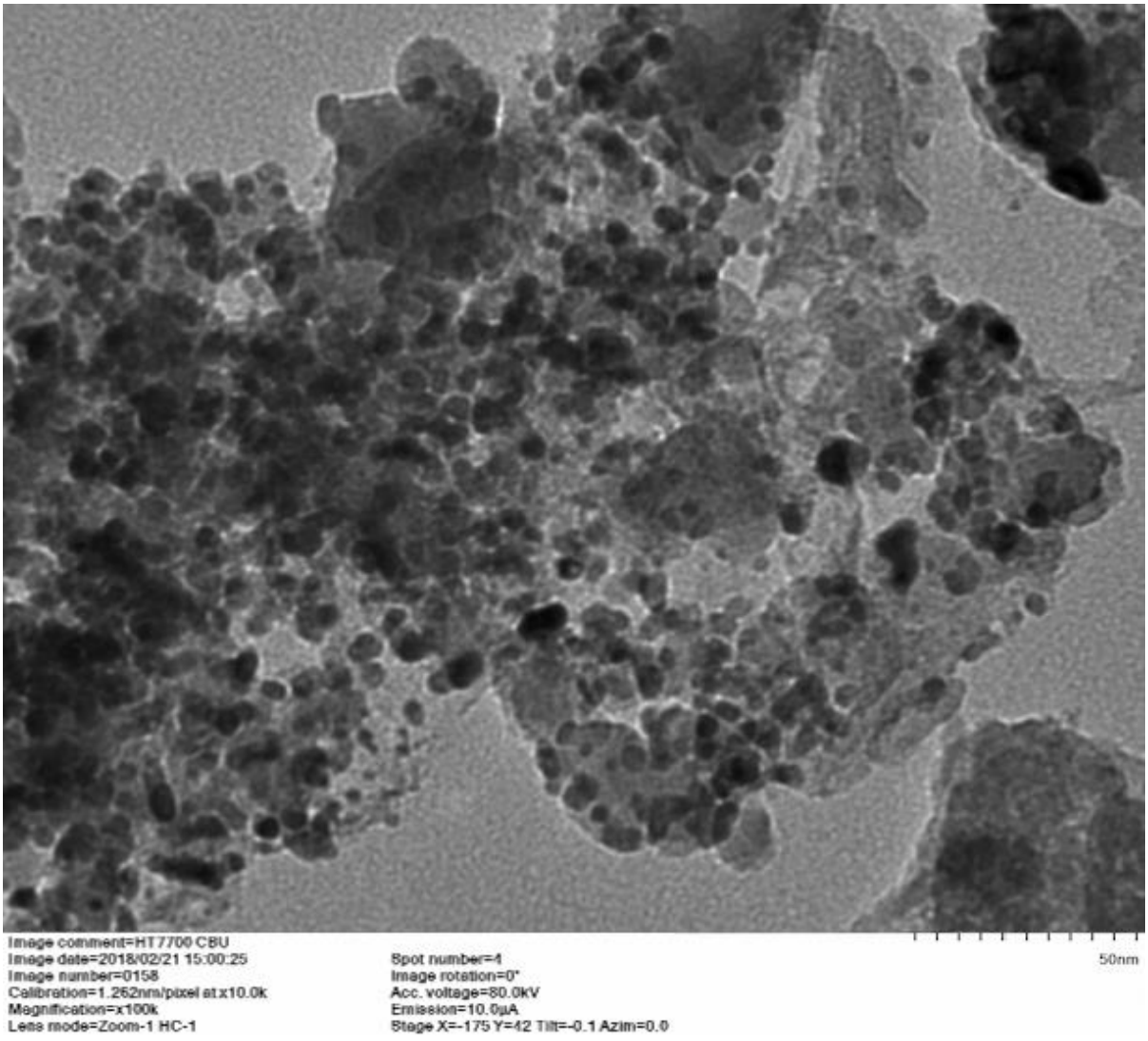

Figure 12 Biochar catalyst (Pd-Zn-$CaCO_3$). Dark round particles are likely palladium and zinc.

The catalyst was also analysed after being used. The TEM image shows similar round particles on the surface of the biochar (figure 16). However, it seems as though the particles are now in clusters that are closer together. This is known as Ostwald ripening. Ostwald ripening is when small nanoparticles are deposited into larger particles to reach a more thermodynamically stable state. These larger particles are essentially immobile and will decrease the activity of the catalyst.[30]

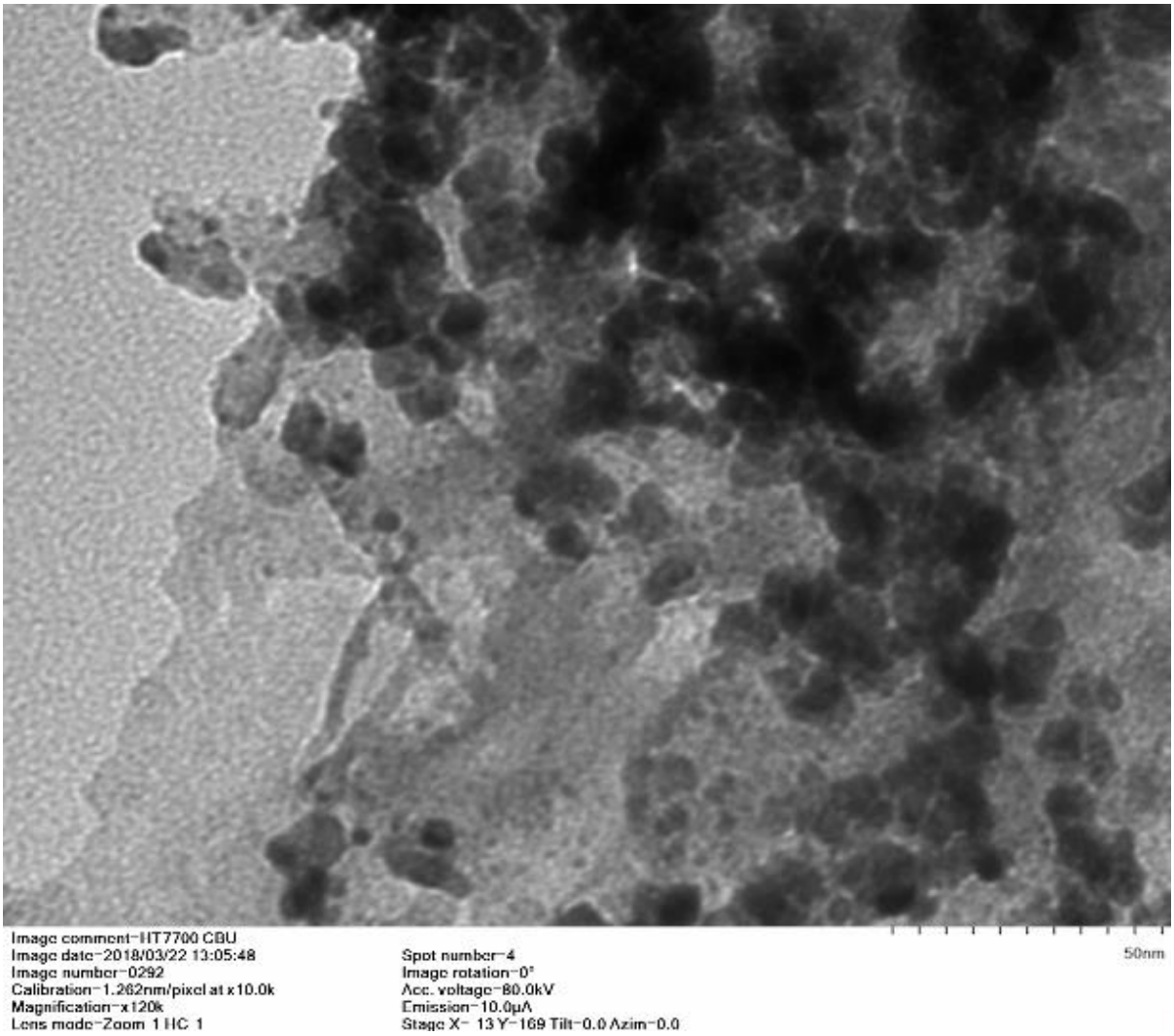

Figure 13 TEM image for Pd-Zn-$CaCO_3$ catalyst after being used in a hydrogenation reaction.

4 Results and Discussion

4.1 $CaCO_3$ Removal

Three different techniques were used to attempt to remove $CaCO_3$. For one technique simple acid-base reaction between HCl and $CaCO_3$ was used. The second technique was to heat the biochar in water at 80. The last technique was to just have the biochar in water. The experiments took place for 48 hours. After the experiment the biochar was filtered, dried, and weighed. The change in mass was assumed to be and $CaCO_3$ removed.

Conditions (48h)	**Temperature (°C)**	**Initial Mass (g)**	**Final Mass (g)**	**Change in Mass (g)**
5 mL H_2O	RT	0.1003	0.0955	0.0048
5 mL H_2O	80	0.1006	0.0954	0.0052
5 mLH_2O +2 ml HCl	RT	0.1007	0.0855	0.0152

Table 2 Results for $CaCO_3$ removal.

The biggest mass loss, 15.2 mg, was seen in the reaction with HCl. This was expected because $CaCO_3$ is not soluble in water. To see if this mass loss was due to the loss of $CaCO_3$ FT-IR was performed on the treated biochar samples (figure 17). The intensity for the $CaCO_3$ bands decreased for all three treatments. This showed that $CaCO_3$ was removed. The bands for CaO are more noticeable in the biochar now.

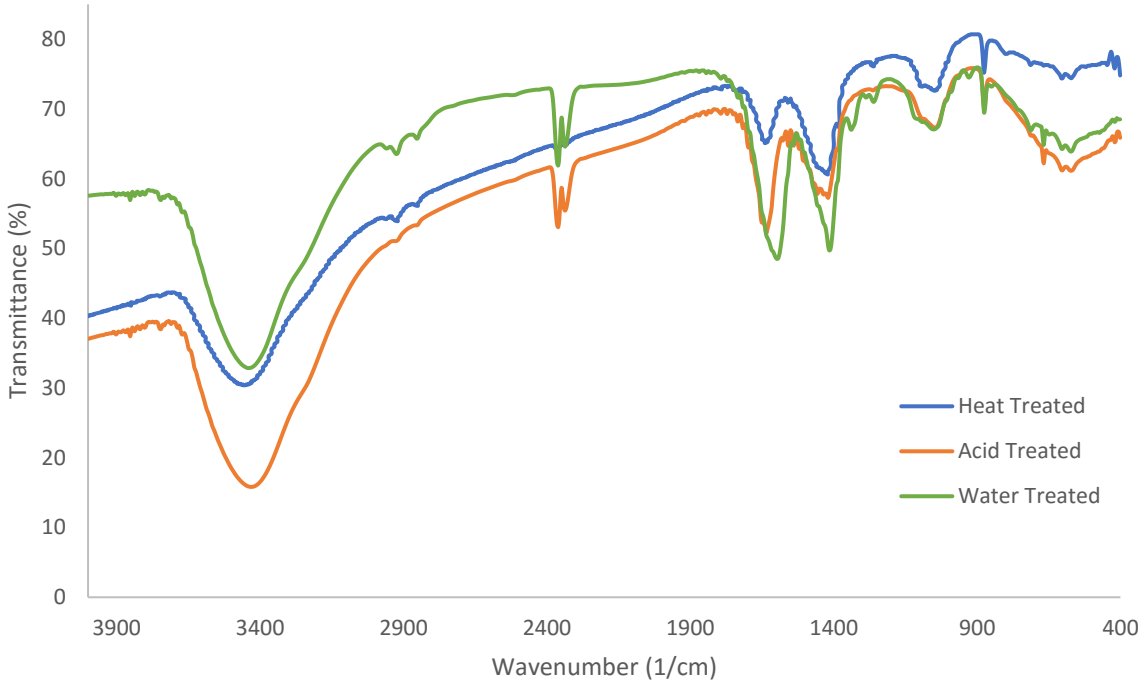

Figure 14 FT-IR for heat treated CRB (blue), water treated CRB (green), and acid treated CRB (orange).

4.2 Soxhlet extraction of CBR

A soxhlet extraction of the crab biochar was preformed to remove any possible contaminants. Roughly 500 mg of crab biochar was placed in 200 mL of ethanol. The extraction took place for 7 hours. The extract was evaporated on a rotary evaporator to remove excess solvent.

An Agilent Technologies 6890N Network GC system was used to obtain gas chromatograms. A J&K Sci 2175-5030 column was used. The column length is 15 m, the diameter is 250.00 μm, and a film thickness of 0.30μm. The carrier gas was nitrogen with a flow rate of 1.0 mL/min. The solvent was ethanol and a 4-minute solvent delay was used. The initial oven temperature was 100°C. The first temperature ramp was to heat the oven to

140°C at a rate of 5°C/min and then held for 5 minutes. Next temperature ramp was to heat the oven to 220°C at a rate of 15°C/min and held for 10 minutes.

A blank run was preformed using 99% anhydrous ethanol (figure 18). One impurity was found in the solvent. From a library search the impurity was found to most likely be 9-octadecenamide, that eluted at 33.274 minutes.

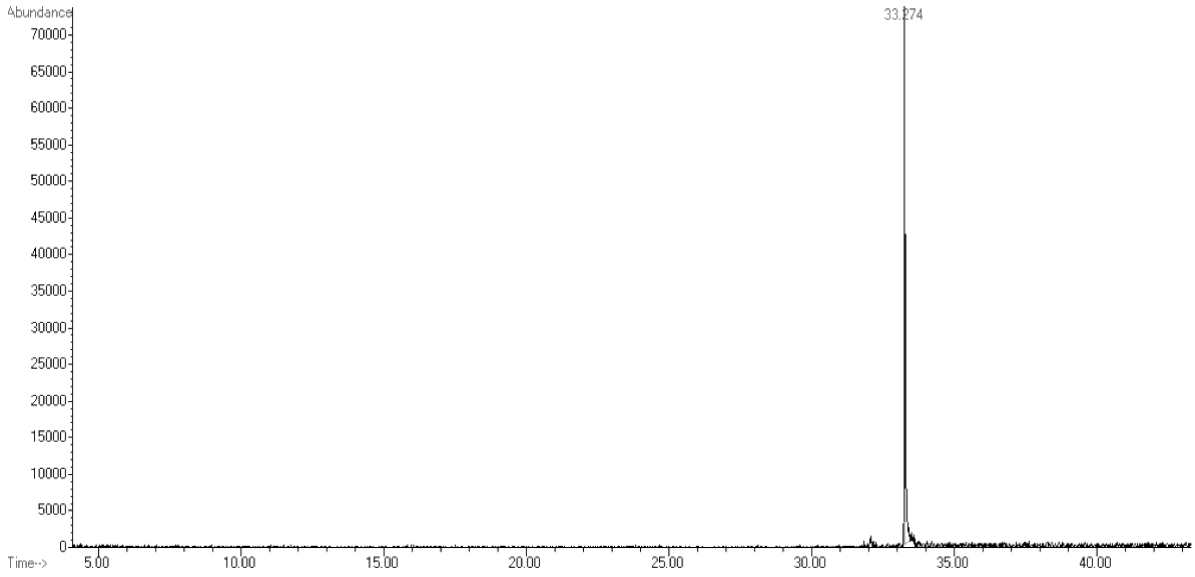

Figure 15 Gas chromatogram for ethanol blank.

The CRB extract analysis showed several impurities (figure 19). A library search was used to determine what possible impurities are present. The most relevant compounds were vanillin at 4.227 minutes, benzophenone at 14.490 minutes, n-hexadecanoic acid at 29.609 minutes, octadecanoic acid ethyl ester at 32.231 minutes, docosane at 32.289 minutes, (Z)-9-octadecenamide at 33.273 minutes, 1, 54-dibromo-tetrapentacotane at 34.120 minutes, hexacosane at 35.414 minutes, heptacosane at 36.712 minutes, tritetracotane 36.935 minutes, heptadecane at 38.439 minutes, eicosane at 38.727, and nonacosane at 40.746 minutes. Most of these compounds are long alkyl chains.

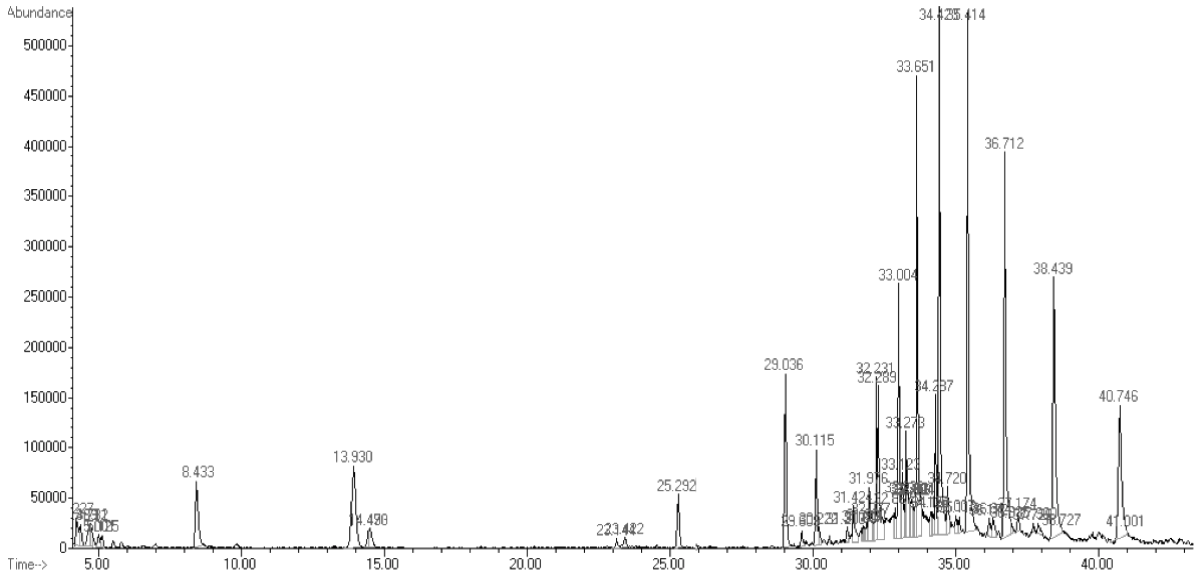

Figure 16 Gas Chromatogram for soxhelt extraction of CRB

4.3 Hydrogenation Reaction

An Agilent Technologies 6890N Network GC system was used to obtain gas chromatograms. A J&K Scientific NSP-1701 column was used. The column length is 20 m, the diameter is 180.00 μm, and a film thickness of 0.18μm. The carrier gas was nitrogen with a flow rate of 1.0 mL/min. The solvent was methanol and a 4-minute solvent delay was used. The initial oven temperature was 70°C. The first temperature ramp was to heat the oven to 140°C at a rate of 5°C/min and then held for 5 minutes. Next temperature ramp was to heat the oven to 220°C at a rate of 15°C/min and held for 10 minutes.

A blank run was preformed using methanol (figure 20). Several impurities were found in the solvent. A library search showed … as the possible impurities. The presence of these impurities were ignored in the gas chromatogram analysis of the hydrogenation reaction.

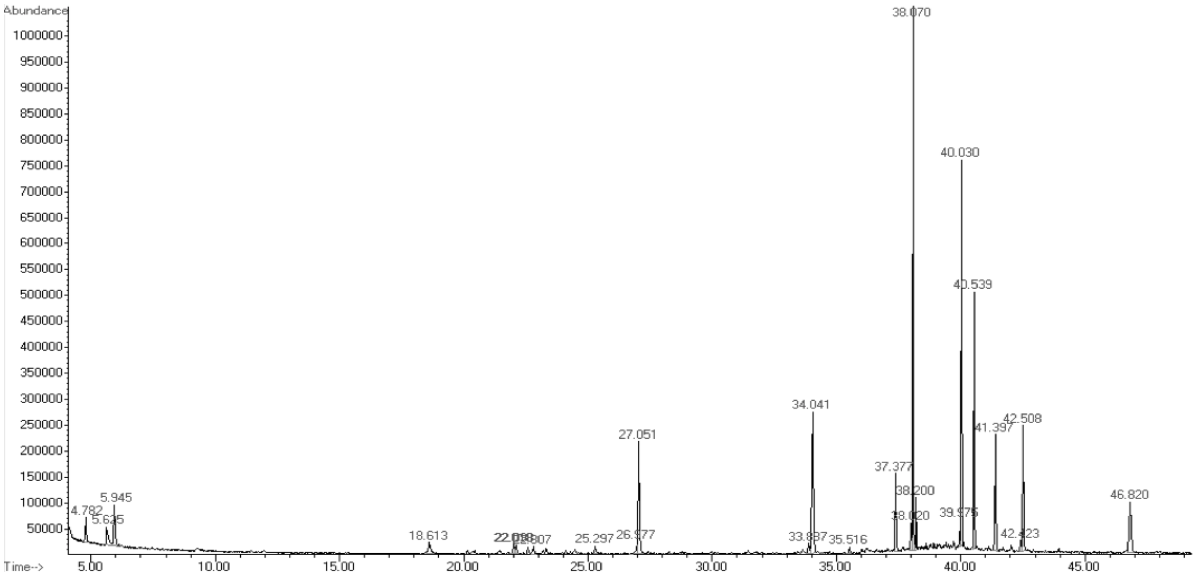

Figure 17 Gas chromatogram for methanol.

The gas chromatogram showed a peak ay 11.630 minutes that is likely 1,4-butanediol (figure 21). This means the Pd-Zn-$CaCO_3$ biochar catalyst successfully worked to hydrogenate 2-butyne-1,4-diol. However, it fully saturate the alkyen to the alkane (scheme 2) instead of stopping at the cis-alkene. The tailing peak shape for 1,4-butanediol is like due to the column used to separate the sample.

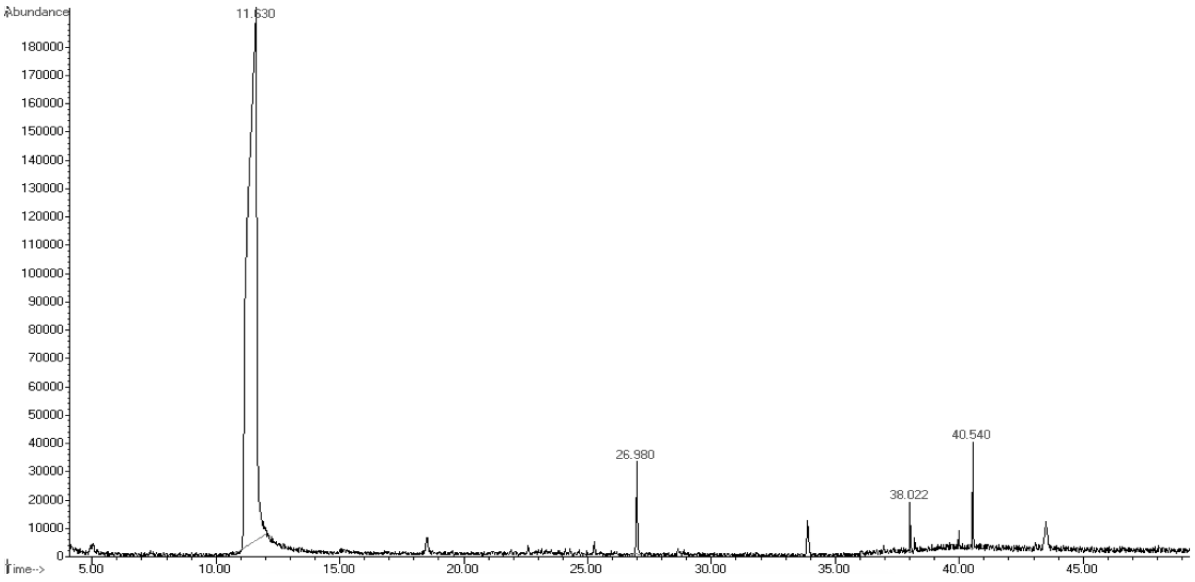

Figure 18 Gas chromatogram for hydrogenation reaction of 2-butyne-1,4-diol using the Pd-Zn supported on $CaCO_3$ in crab biochar catalyst.

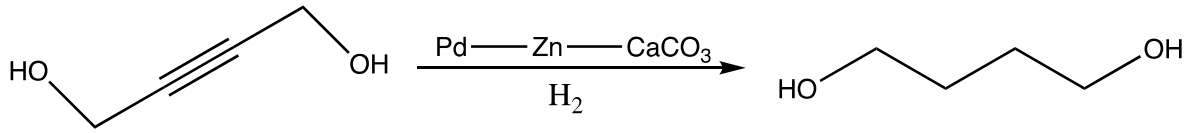

Scheme 2 Hydrogenation of 2-butyne-1,4-diol to butane-1,4-diol catalyzed by Pd-Zn-$CaCO_3$.

As a comparison the same Pd-Zn-$CaCO_3$ catalyst using pure $CaCO_3$ was developed. This is the same as the catalyst generated by Chaudhari, R. V. et al.[24] Similarly this catalyst was supposed to hydrogenate 2-butyen-1,4-diol to cis-2-butene-1,4-diol. However, like the Pd-Zn-$CaCO_3$ crab biochar catalyst, the alkyne became fully saturated. The main difference seen in the chromatogram is not all the 2-butyne-1,4-diol was reacted. The peak at 12.571 minutes is likely due to 2-butyen-1,4-diol.

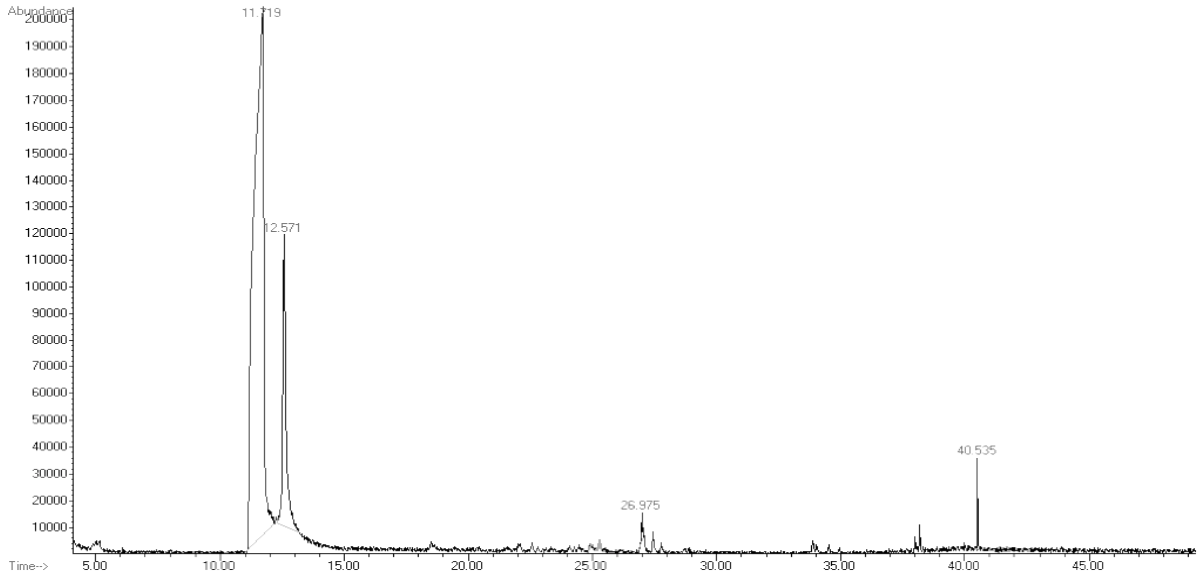

Figure 19 Gas chromatogram for hydrogenation reaction of 2-butyne-1,4-diol using the Pd-Zn supported on pure $CaCO_3$ catalyst.

To make sure the palladium is what is responsible for the hydrogenation of 2-butyne-1,4-diol the reaction was attempted using just crab biochar. The peak at 18.013 minutes is indicative of 2-butyne-1,4-diol eluting (figure 22). This shows the palladium needs to be present on the biochar to act as a catalyst.

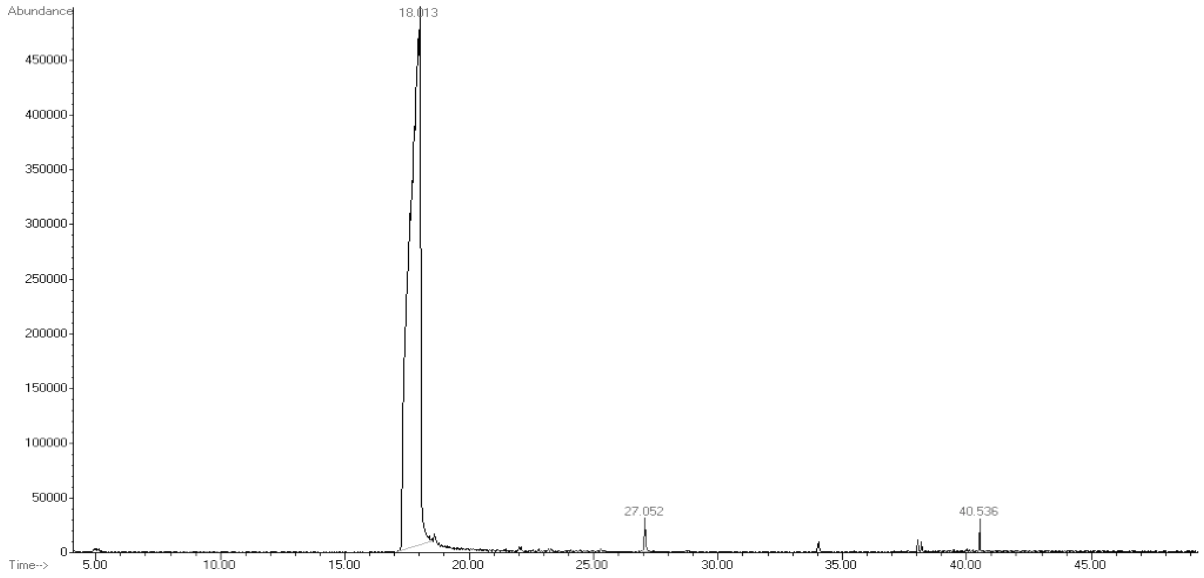

Figure 20 Gas chromatogram for hydrogenation reaction of 2-butyne-1,4-diol using the untreated crab biochar.

5 Conclusion

Biochar was generated from crab bodies obtained from Louisbourg Seafoods Ldt. The biochar was characterized by FT-IR, XRD, TEM, BET, and elemental analysis. The biochar was found to contain a significant $CaCO_3$ content from FT-IR and XRD. The surface area of the biochar was found to be 16.3 m^2/g. TEM images showed that the biochar contains some ordered regions as well as some amorphous regions.

The crab biochar was treated with palladium and zinc to successfully generate a Pd-Zn-$CaCO_3$ catalyst. This catalyst was hypothesized to hydrogenate 2-butyne-1,4-diol to cis-2-butene-1,4-diol. However, the alkyne diol was completely hydrogenated to the alkane. So it was likely that zinc was not a good enough poison to stop the catalyst. Also the palladium could have been added directly onto the carbon in the biochar rather than the $CaCO_3$. This would also have negative impacts on the poisoning of the catalyst.

In further work the use of the Pd-Zn-$CaCO_3$ catalyst should be optimized. Studying how the catalyst can be modified to only hydrogenate to the cis-alkene compound, as well as investigation of different poisons. Also, a study should be performed to see if the catalyst can be recycled.

6 References

(1) Pinfold, G. Overview of the Atlantic Snow Crab Industry. *Submitt. Dep. Fish. Oceans* **2006**.

(2) Davidson, K.; Roff, J. C.; Elner, R. W. Morphological, Electrophoretic and Fecundity Characteristics of Atlantic Snow Crab, Chionoecetes Opilio, and Implications for Fisheries Management. *Can. J. Fish. Aquat. Sci.* **1985**, *42* (3), 474–482.

(3) Government of Canada. Canada's Fisheries Fast Facts 2016.

(4) Dai, L.; Tan, F.; Li, H.; Zhu, N.; He, M.; Zhu, Q.; Hu, G.; Wang, L.; Zhao, J. Calcium-Rich Biochar from the Pyrolysis of Crab Shell for Phosphorus Removal. *J. Environ. Manage.* **2017**, *198*, 70–74.

(5) Kerton, F. M.; Liu, Y.; Omari, K. W.; Hawboldt, K. Green Chemistry and the Ocean-Based Biorefinery. *Green Chem.* **2013**, *15* (4), 860.

(6) Xiao, Y.; Xue, Y.; Gao, F.; Mosa, A. Sorption of Heavy Metal Ions onto Crayfish Shell Biochar: Effect of Pyrolysis Temperature, PH and Ionic Strength. *J. Taiwan Inst. Chem. Eng.* **2017**.

(7) Magnacca, G.; Guerretta, F.; Vizintin, A.; Benzi, P.; Valsania, M. C.; Nisticò, R. Preparation, Characterization and Environmental/Electrochemical Energy Storage Testing of Low-Cost Biochar from Natural Chitin Obtained via Pyrolysis at Mild Conditions. *Appl. Surf. Sci.* **2018**, *427*, 883–893.

(8) Duan, S.; Li, L.; Zhuang, Z.; Wu, W.; Hong, S.; Zhou, J. Improved Production of Chitin from Shrimp Waste by Fermentation with Epiphytic Lactic Acid Bacteria. *Carbohydr. Polym.* **2012**, *89* (4), 1283–1288.

(9) Faatz, M.; Gröhn, F.; Wegner, G. Amorphous Calcium Carbonate: Synthesis and Potential Intermediate in Biomineralization. *Adv. Mater.* **2004**, *16* (12), 996–1000.

(10) Hammes, F.; Verstraete, W. Key Roles of PH and Calcium Metabolism in Microbial Carbonate Precipitation. *Rev. Environ. Sci. Biotechnol.* **2002**, *1* (1), 3–7.

(11) Gower, L. B.; Odom, D. J. Deposition of Calcium Carbonate Films by a Polymer-Induced Liquid-Precursor (PILP) Process. *J. Cryst. Growth* **2000**, *210* (4), 719–734.

(12) Meldrum, F. C. Calcium Carbonate in Biomineralisation and Biomimetic Chemistry. *Int. Mater. Rev.* **2003**, *48* (3), 187–224.

(13) Crombie, K.; Mašek, O.; Sohi, S. P.; Brownsort, P.; Cross, A. The Effect of Pyrolysis Conditions on Biochar Stability as Determined by Three Methods. *GCB Bioenergy* **2013**, *5* (2), 122–131.

(14) Kwapinski, W.; Byrne, C. M. P.; Kryachko, E.; Wolfram, P.; Adley, C.; Leahy, J. J.; Novotny, E. H.; Hayes, M. H. B. Biochar from Biomass and Waste. *Waste Biomass Valorization* **2010**, *1* (2), 177–189.

(15) Bamdad, H.; Hawboldt, K.; MacQuarrie, S. A Review on Common Adsorbents for Acid Gases Removal: Focus on Biochar. *Renew. Sustain. Energy Rev.* **2017**.

(16) Ghani, W. A. W. A. K.; Mohd, A.; da Silva, G.; Bachmann, R. T.; Taufiq-Yap, Y. H.; Rashid, U.; Al-Muhtaseb, A. H. Biochar Production from Waste Rubber-Wood-Sawdust and Its Potential Use in C Sequestration: Chemical and Physical Characterization. *Ind. Crops Prod.* **2013**, *44*, 18–24.

(17) Yao, Y.; Gao, B.; Chen, J.; Yang, L. Engineered Biochar Reclaiming Phosphate from Aqueous Solutions: Mechanisms and Potential Application as a Slow-Release Fertilizer. *Environ. Sci. Technol.* **2013**, *47* (15), 8700–8708.

(18) Mohan, D.; Pittman, C. U.; Bricka, M.; Smith, F.; Yancey, B.; Mohammad, J.; Steele, P. H.; Alexandre-Franco, M. F.; Gómez-Serrano, V.; Gong, H. Sorption of Arsenic, Cadmium, and Lead by Chars Produced from Fast Pyrolysis of Wood and Bark during Bio-Oil Production. *J. Colloid Interface Sci.* **2007**, *310* (1), 57–73.

(19) Shafeeyan, M. S.; Daud, W. M. A. W.; Houshmand, A.; Shamiri, A. A Review on Surface Modification of Activated Carbon for Carbon Dioxide Adsorption. *J. Anal. Appl. Pyrolysis* **2010**, *89* (2), 143–151.

(20) Plaza, M. G.; Pevida, C.; Pis, J. J.; Rubiera, F. Evaluation of the Cyclic Capacity of Low-Cost Carbon Adsorbents for Post-Combustion CO2 Capture. *Energy Procedia* **2011**, *4*, 1228–1234.

(21) Zhang, X.; Zhang, S.; Yang, H.; Feng, Y.; Chen, Y.; Wang, X.; Chen, H. Nitrogen Enriched Biochar Modified by High Temperature CO2–ammonia Treatment: Characterization and Adsorption of CO2. *Chem. Eng. J.* **2014**, *257*, 20–27.

(22) Boey, P.-L.; Maniam, G. P.; Hamid, S. A. Biodiesel Production via Transesterification of Palm Olein Using Waste Mud Crab (Scylla Serrata) Shell as a Heterogeneous Catalyst. *Bioresour. Technol.* **2009**, *100* (24), 6362–6368.

(23) Suppes, G. J.; Bockwinkel, K.; Lucas, S.; Botts, J. B.; Mason, M. H.; Heppert, J. A. Calcium Carbonate Catalyzed Alcoholysis of Fats and Oils. *J. Am. Oil Chem. Soc.* **2001**, *78* (2), 139–146.

(24) Chaudhari, R. V.; Parande, M. G.; Ramachandran, P. A.; Brahme, P. H.; Vadgaonkar, H. G.; Jaganathan, R. Hydrogenation of Butynediol to Cis-Butenediol Catalyzed by Pd-Zn-CaCO3: Reaction Kinetics and Modeling of a Batch Slurry Reactor. *AIChE J.* **1985**, *31* (11), 1891–1903.

(25) Stachurski, J.; Thomas, J. M. Structural Aspects of the Lindlar Catalyst for Selective Hydrogenation. *Catal. Lett.* **1988**, *1* (1–3), 67–72.

(26) Lindlar, H.; Dubuis, R. Palladium Catalyst for Partial Reduction of Acetylenes. *Org. Synth.* **1966**, *46*, 89.

(27) Oladoja, N. A.; Raji, I. O.; Olaseni, S. E.; Onimisi, T. D. In Situ Hybridization of Waste Dyes into Growing Particles of Calcium Derivatives Synthesized from a Gastropod Shell (Achatina Achatina). *Chem. Eng. J.* **2011**, *171* (3), 941–950.

(28) Kontoyannis, C. G.; Vagenas, N. V. Calcium Carbonate Phase Analysis Using XRD and FT-Raman Spectroscopy. *The Analyst* **2000**, *125* (2), 251–255.

(29) Schlägl, R.; Noack, K.; Zbinden, H.; Reller, A. The Microstructure of Selective Palladium Hydrogenation Catalysts Supported on Calcium Carbonate and Modified by Lead (*Lindlar* Catalysts), Studied by Photoelectron Spectroscopy, Thermogravimetry, X-Ray Diffraction, and Electron Microscopy. *Helv. Chim. Acta* **1987**, *70* (3), 627–679.

(30) Hansen, T. W.; DeLaRiva, A. T.; Challa, S. R.; Datye, A. K. Sintering of Catalytic Nanoparticles: Particle Migration or Ostwald Ripening? *Acc. Chem. Res.* **2013**, *46* (8), 1720–1730.

7 Appendix

7.1 TEM images

7.1.1 Crab biochar

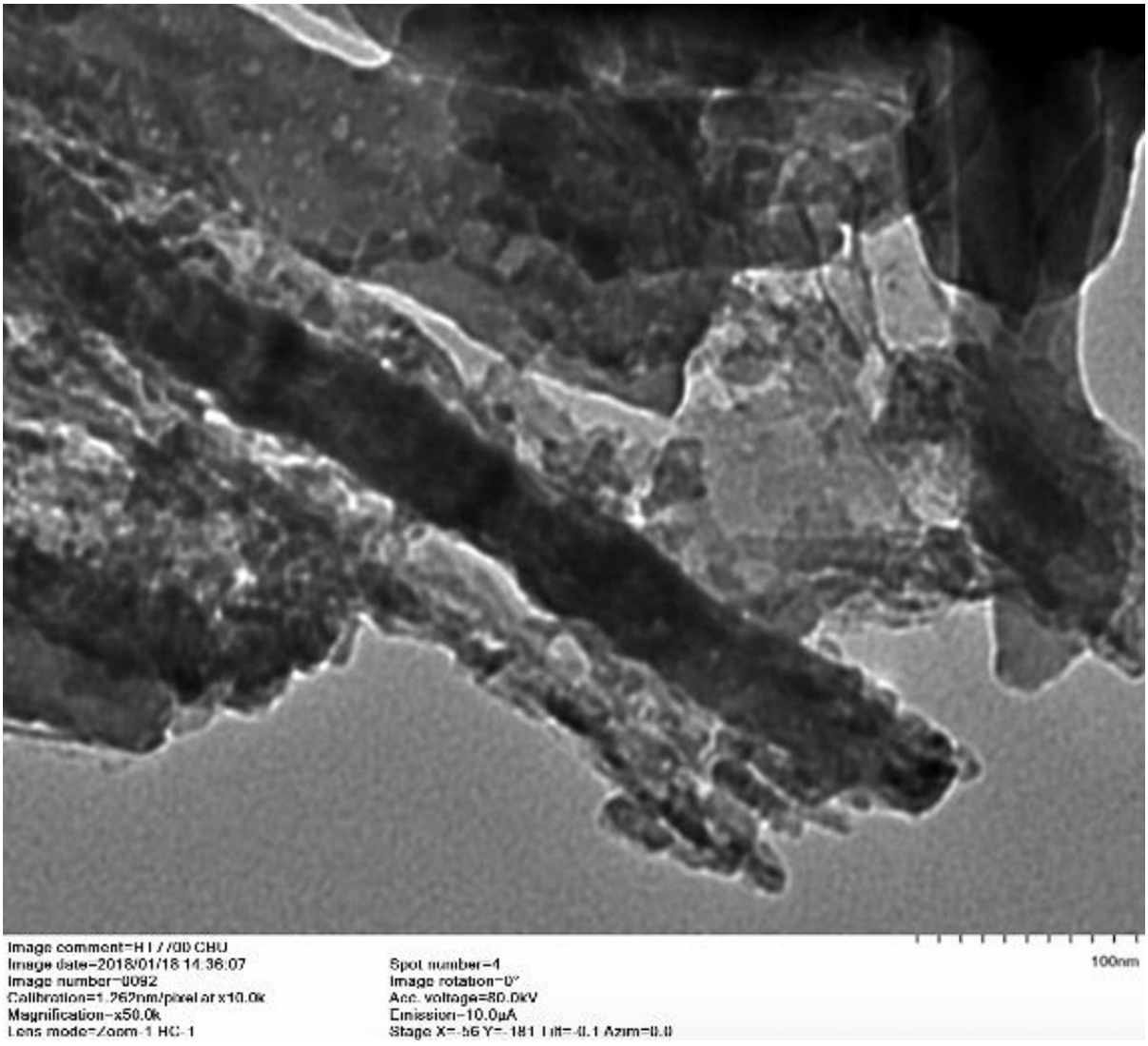

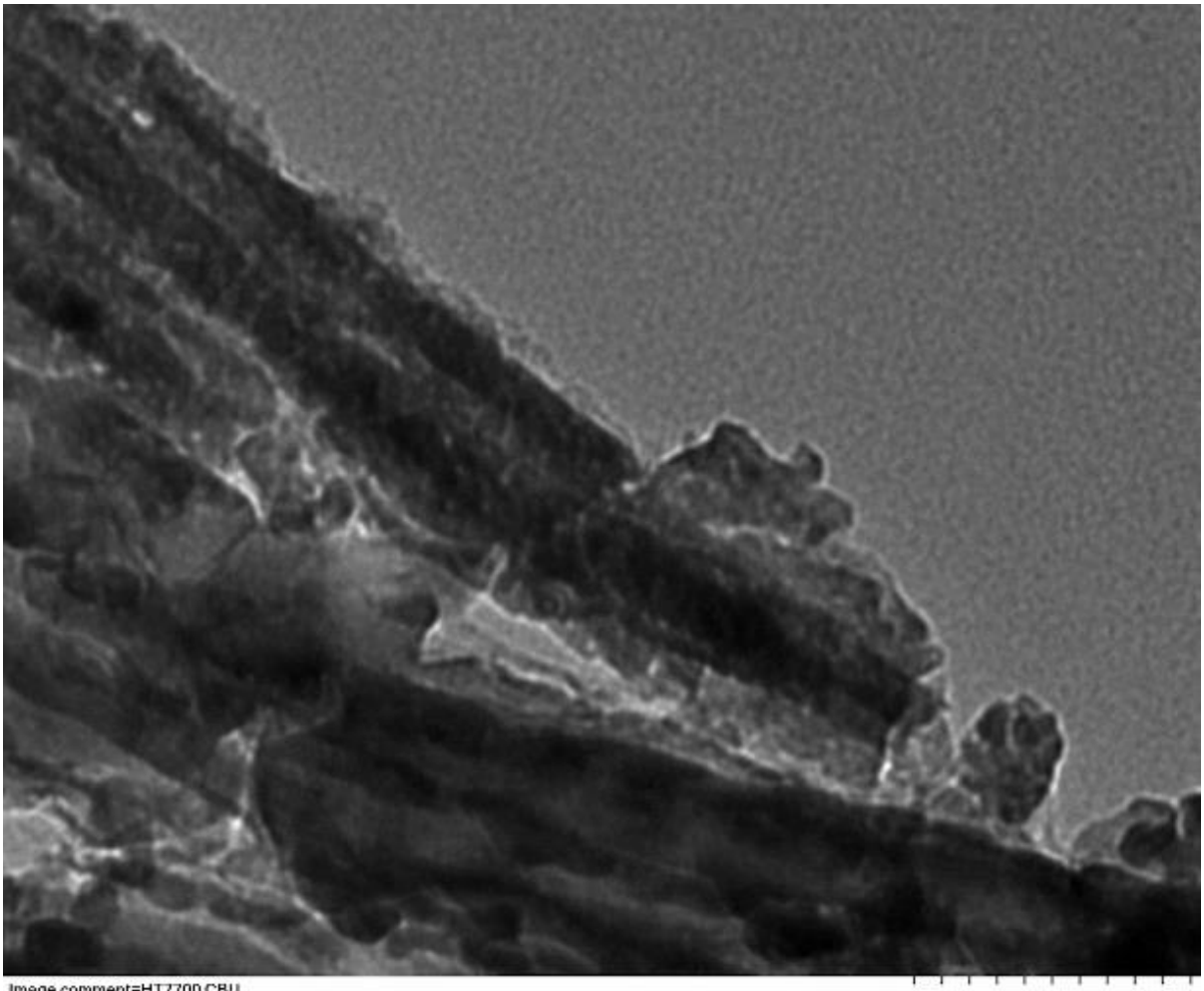

Image comment=HT7700 CBU
Image date=2018/01/18 13:54:12
Image number=0087
Calibration=1.252nm/pixel at x10.0k
Magnification=x60.0k
Lens mode=Zoom-1 HC-1

Spot number=1
Image rotation=0°
Acc. voltage=80.0kV
Emission=10.0μA
Stage X=-85 Y=-117 Tilt=0.2 Azim=0.0

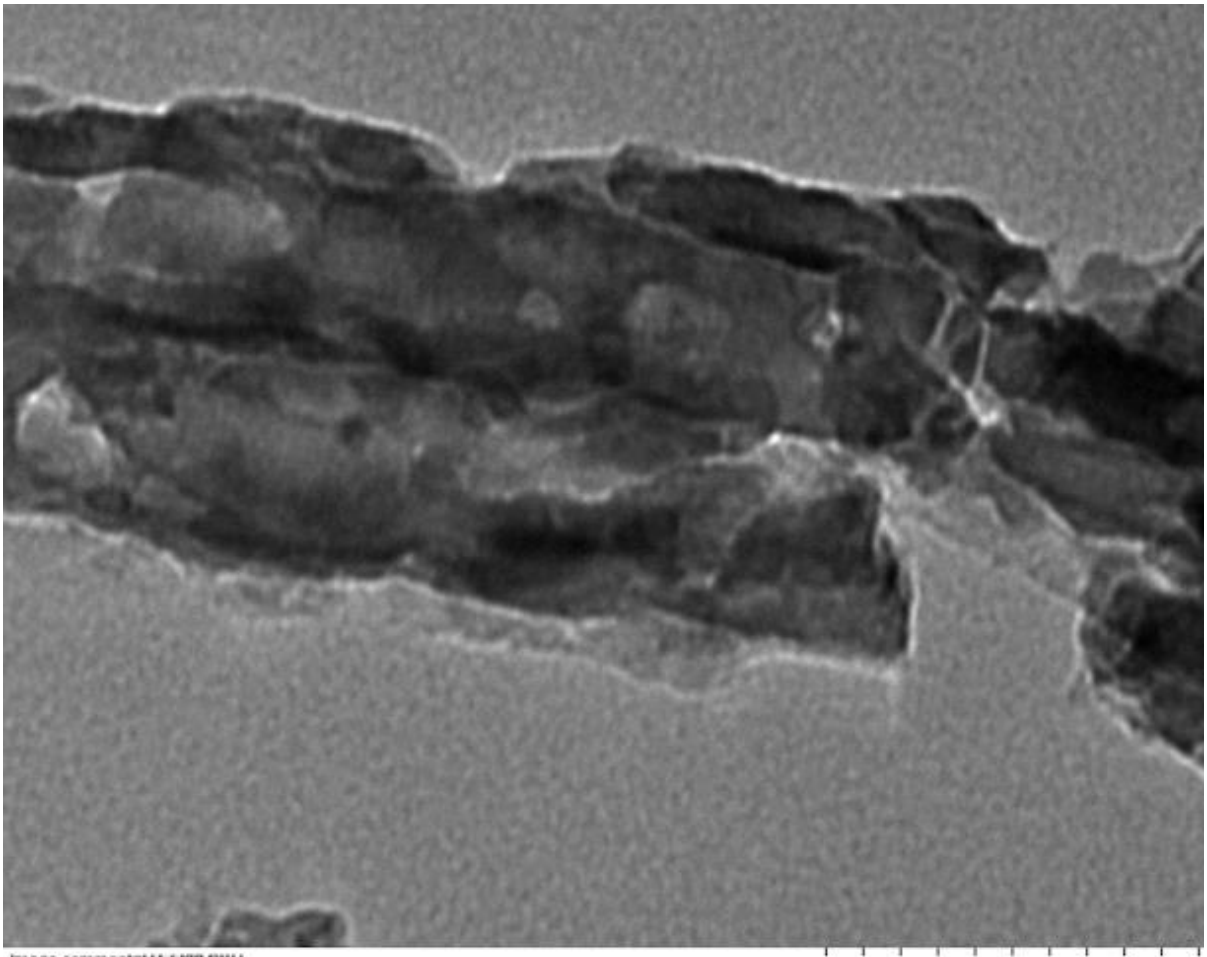
Image comment=H I / /00 C8U
Image date=2018/01/18 14:07:36
Image number=0088
Calibration=1.262nm/pixel at x10.0k
Magnification=x80.0k
Lens mode=Zoom-1 HC-1
Spot number=4
Image rotation=0°
Acc. voltage=80.0kV
Emission=10.0μA
Stage X=-56 Y=-161 Tilt=-0.1 Azim=0.0
100nm

7.1.2 Forestry Crab Biochar Mixture

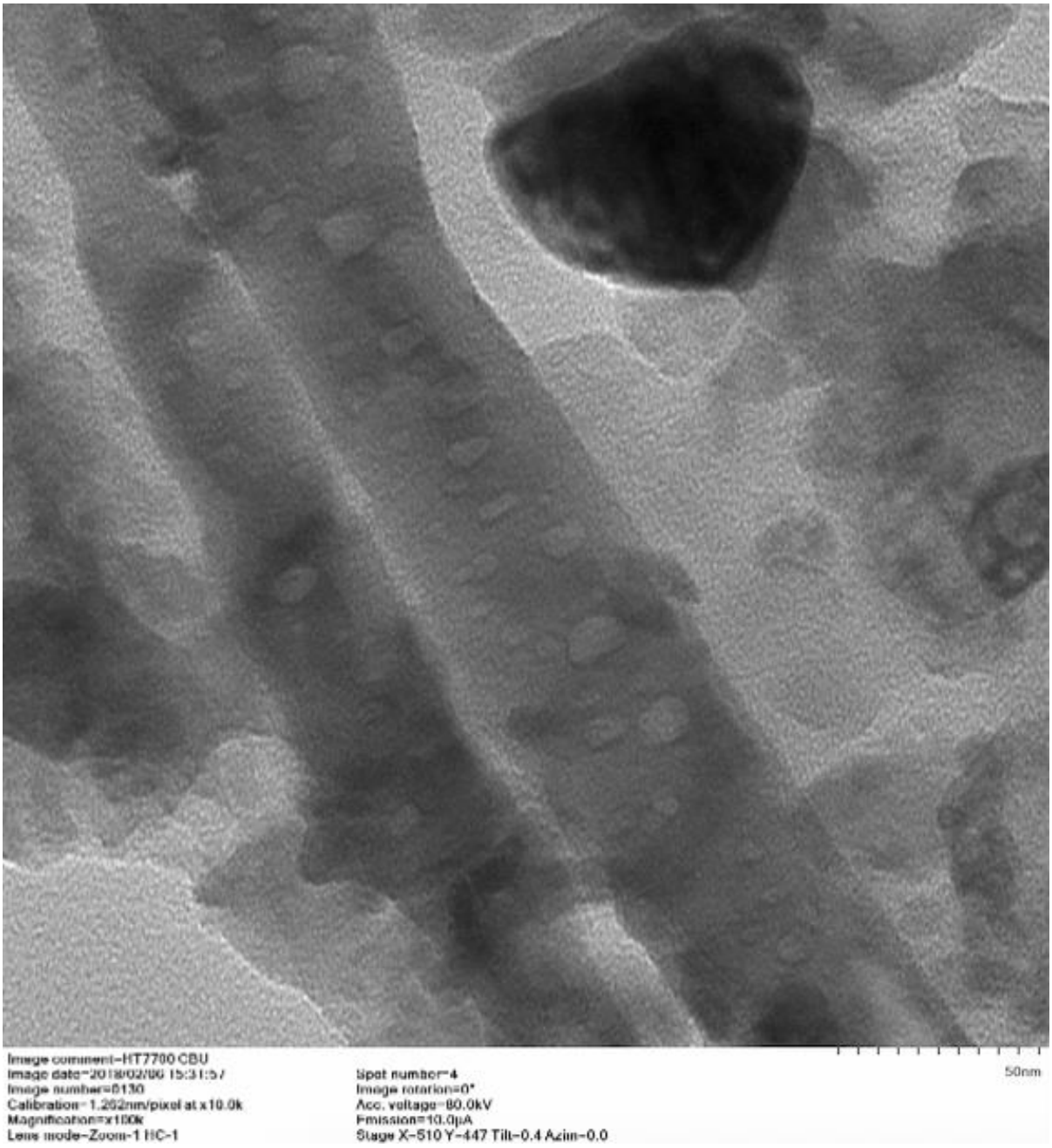

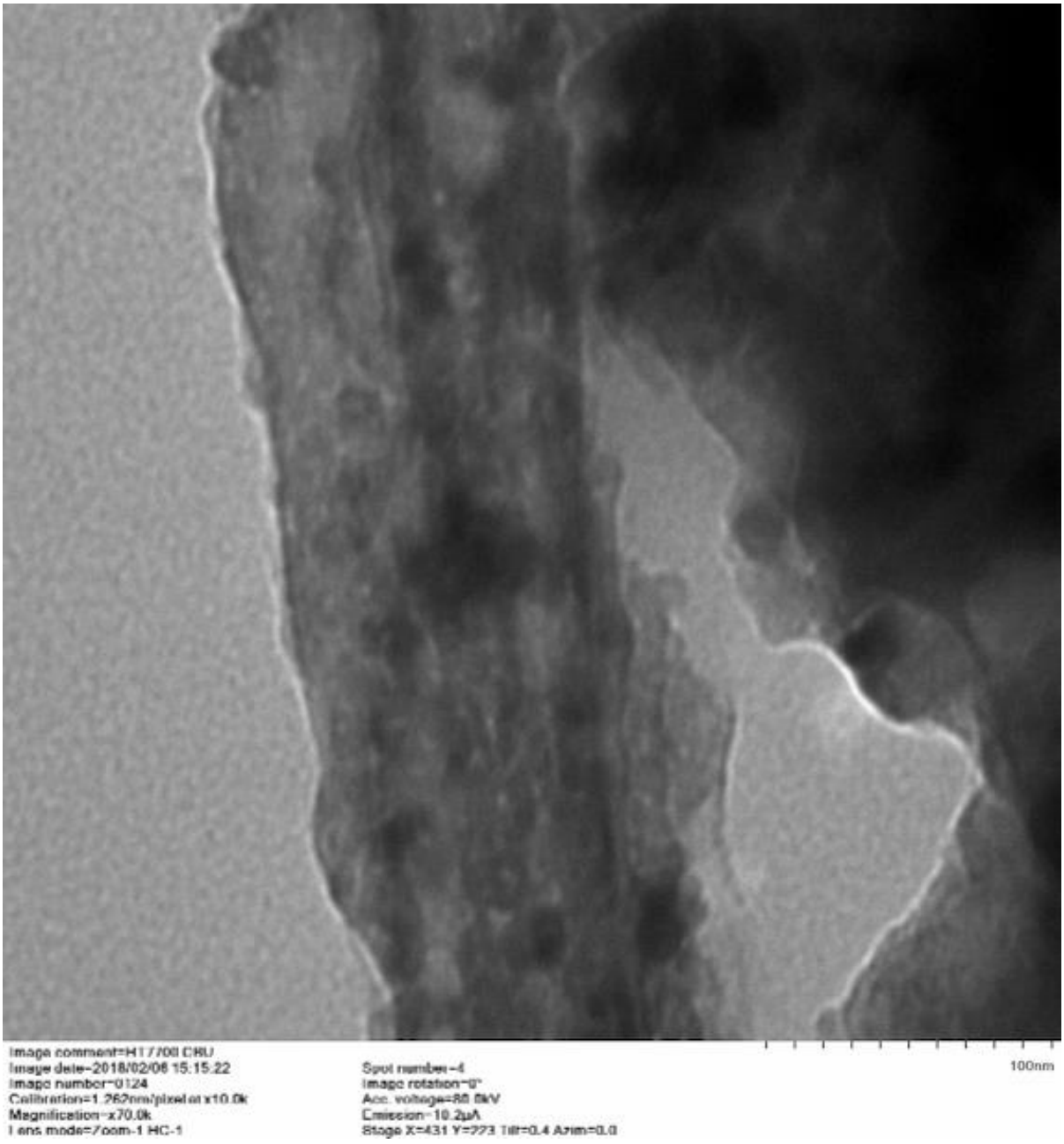
Image comment=H17/00 CRU
Image date=2018/02/06 15:15:22
Image number=0124
Calibration=1.262nm/pixel at x10.0k
Magnification=x70.0k
Lens mode=Zoom-1 HC-1
Spot number=4
Image rotation=0°
Acc. voltage=80.0kV
Emission=10.2μA
Stage X=431 Y=273 Tilt=0.4 Azim=0.0
100nm

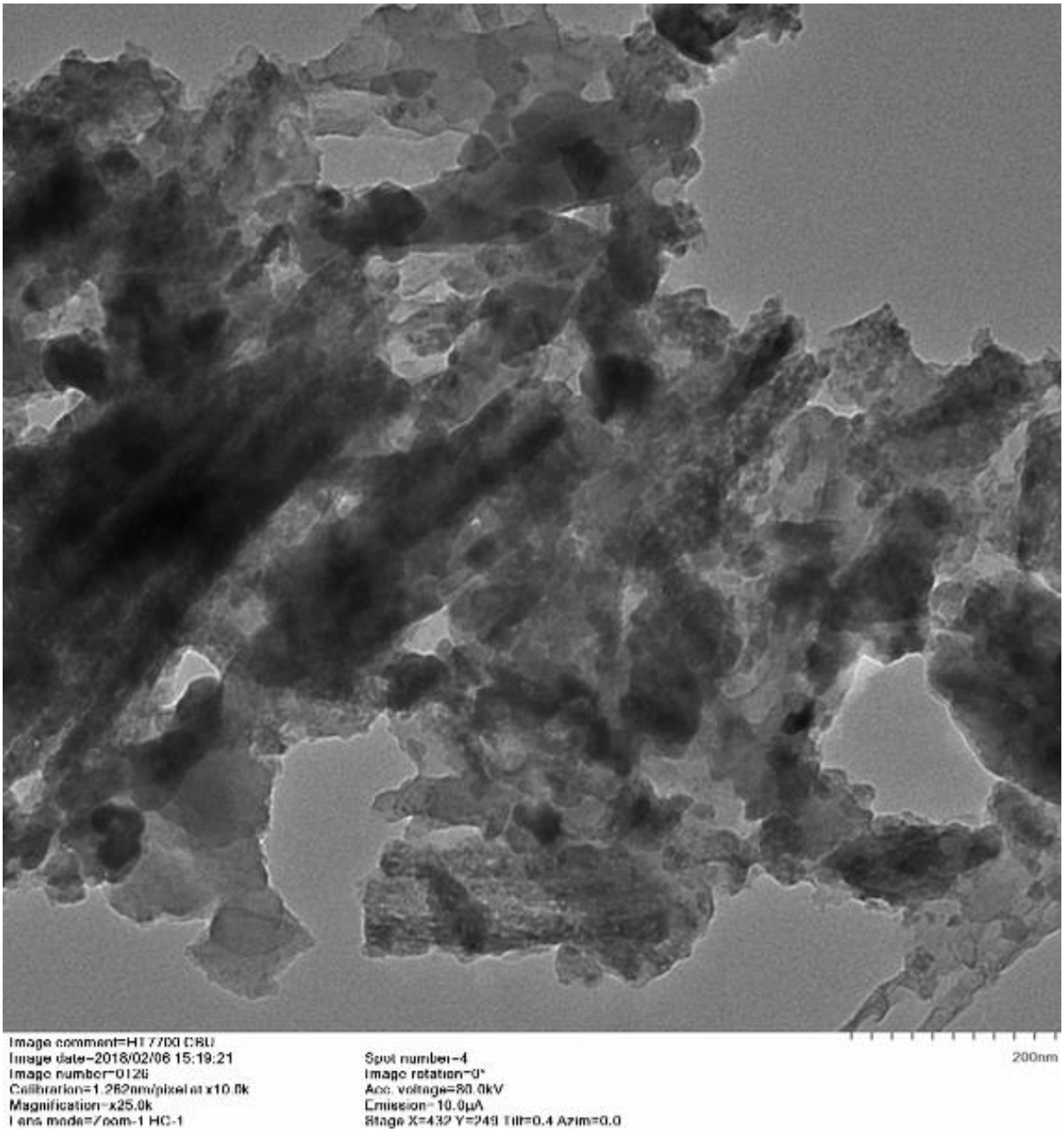
Image comment=HT7700 CBU
Image date=2018/02/06 15:19:21
Image number=0126
Calibration=1.262nm/pixel at x10.0k
Magnification=x25.0k
Lens mode=Zoom-1 HC-1
Spot number=4
Image rotation=0°
Acc. voltage=80.0kV
Emission=10.0μA
Stage X=432 Y=249 Tilt=0.4 Azim=0.0
200nm

7.1.3 Dehydrated Crab Bodies

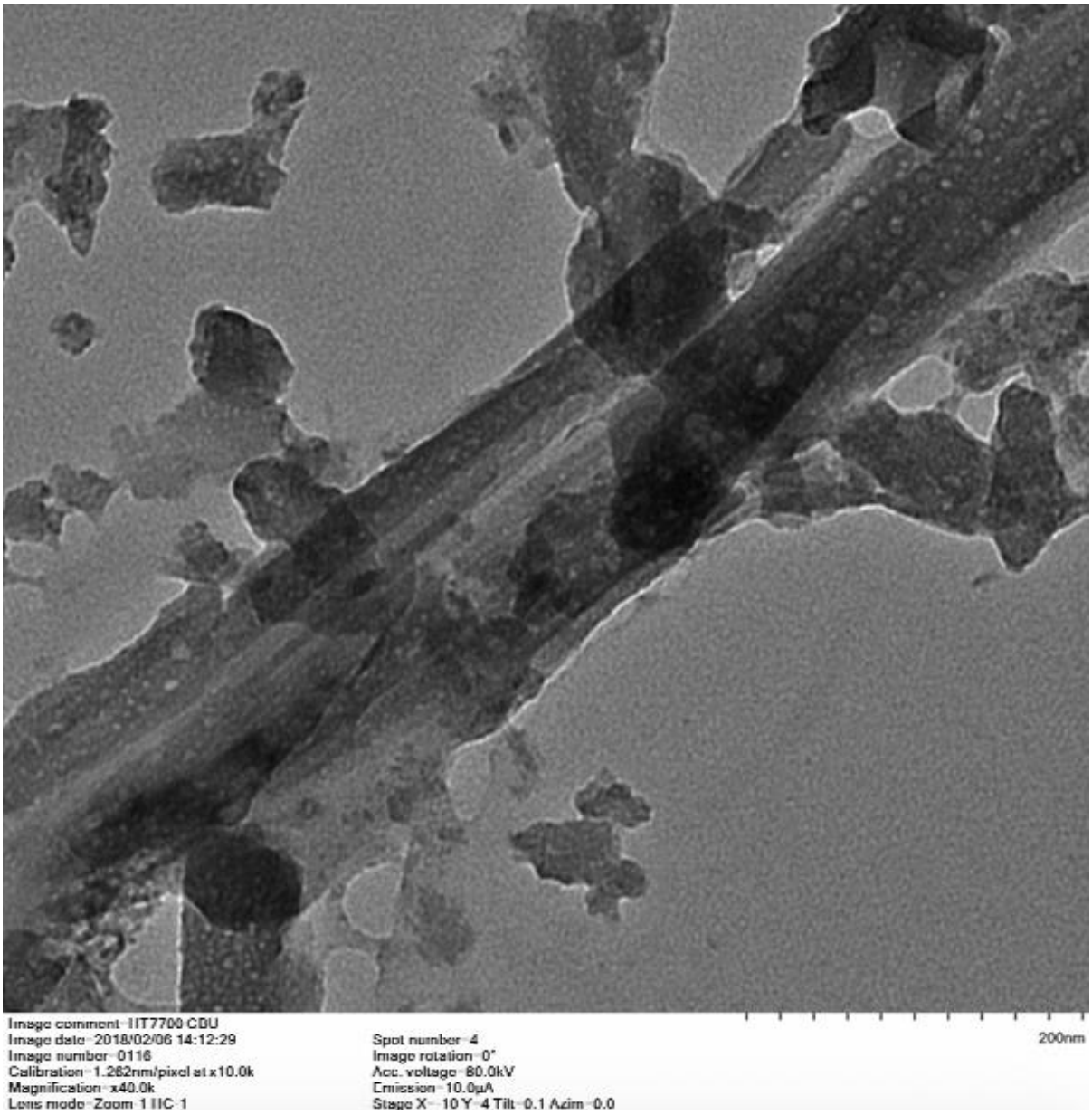

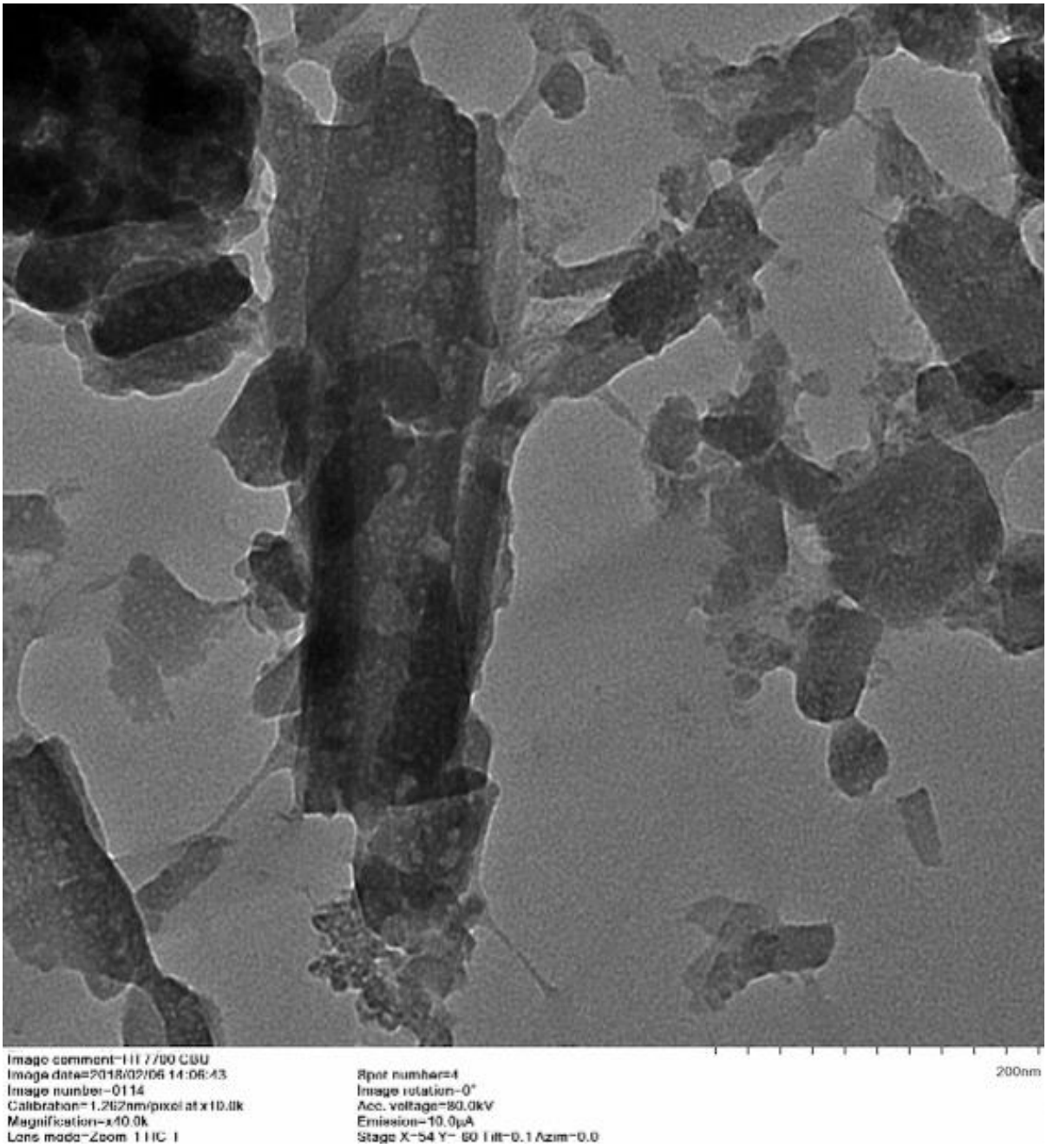
Image comment=HT 7700 C6U
Image date=2018/02/06 14:06:43
Image number=0114
Calibration=1.262nm/pixel at x10.0k
Magnification=x10.0k
Lens mode=Zoom HC 1
Spot number=4
Image rotation=0°
Acc. voltage=80.0kV
Emission=10.0μA
Stage X=54 Y=-60 Tilt=0.1 Azim=0.0
200nm

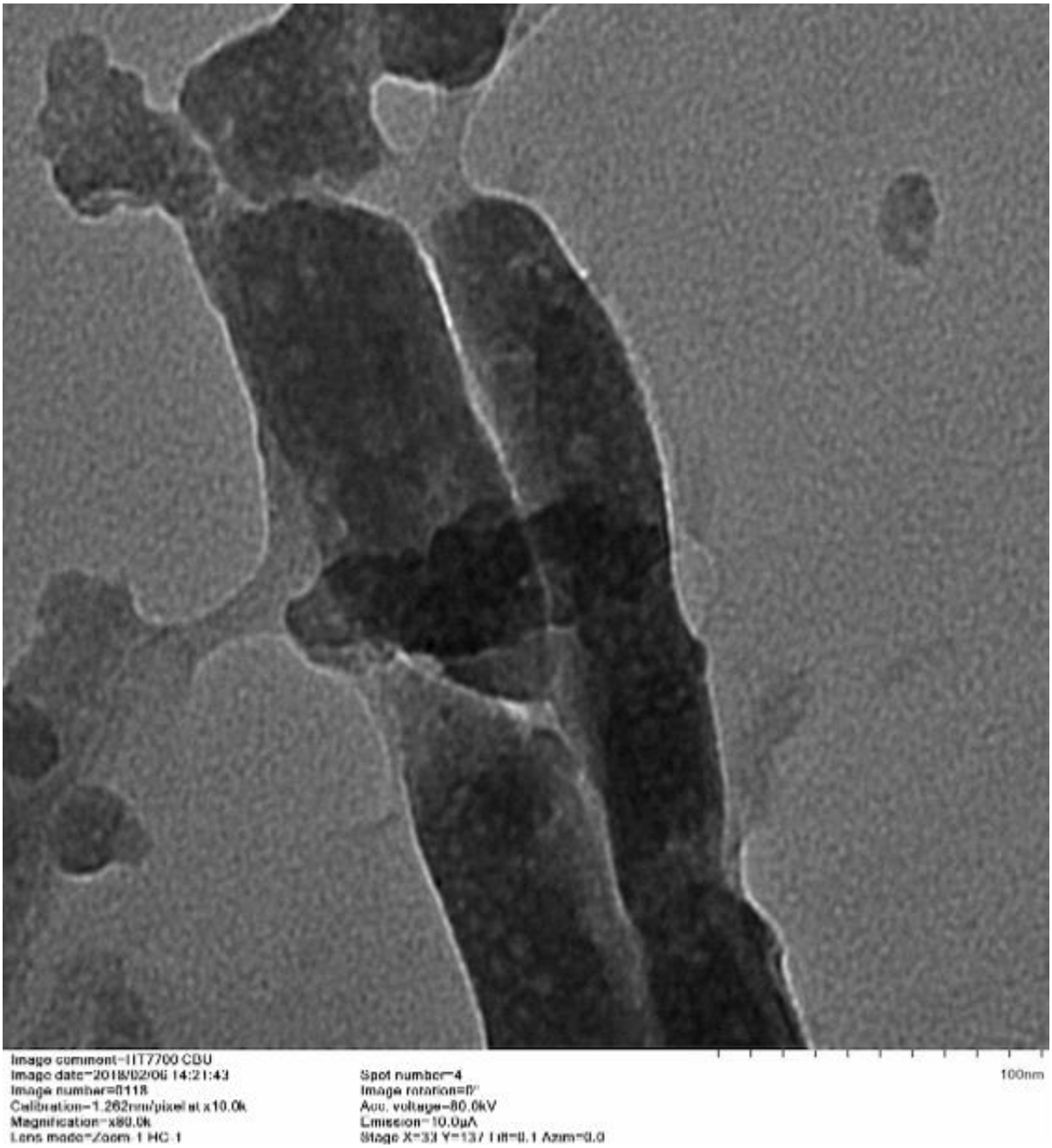
Image comment=HT7700 CBU
Image date=2018/02/06 14:21:43
Image number=0118
Calibration=1.262nm/pixel at x10.0k
Magnification=x80.0k
Lens mode=Zoom 1 HC 1
Spot number=4
Image rotation=0°
Acc. voltage=80.0kV
Emission=10.0μA
Stage X=33 Y=137 Tilt=0.1 Azim=0.0
100nm

7.1.4 Crab Biochar Catalyst Before Use

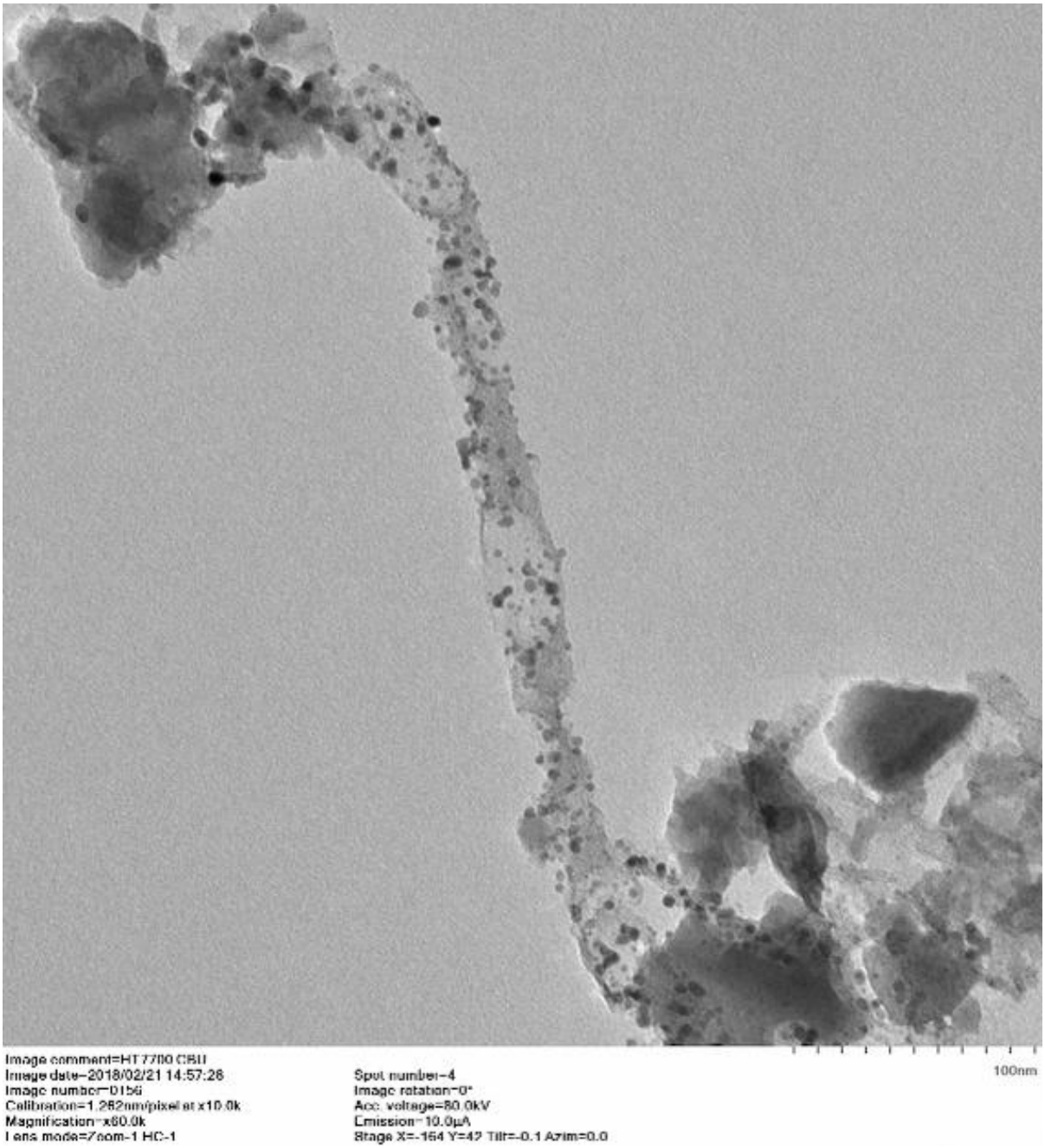

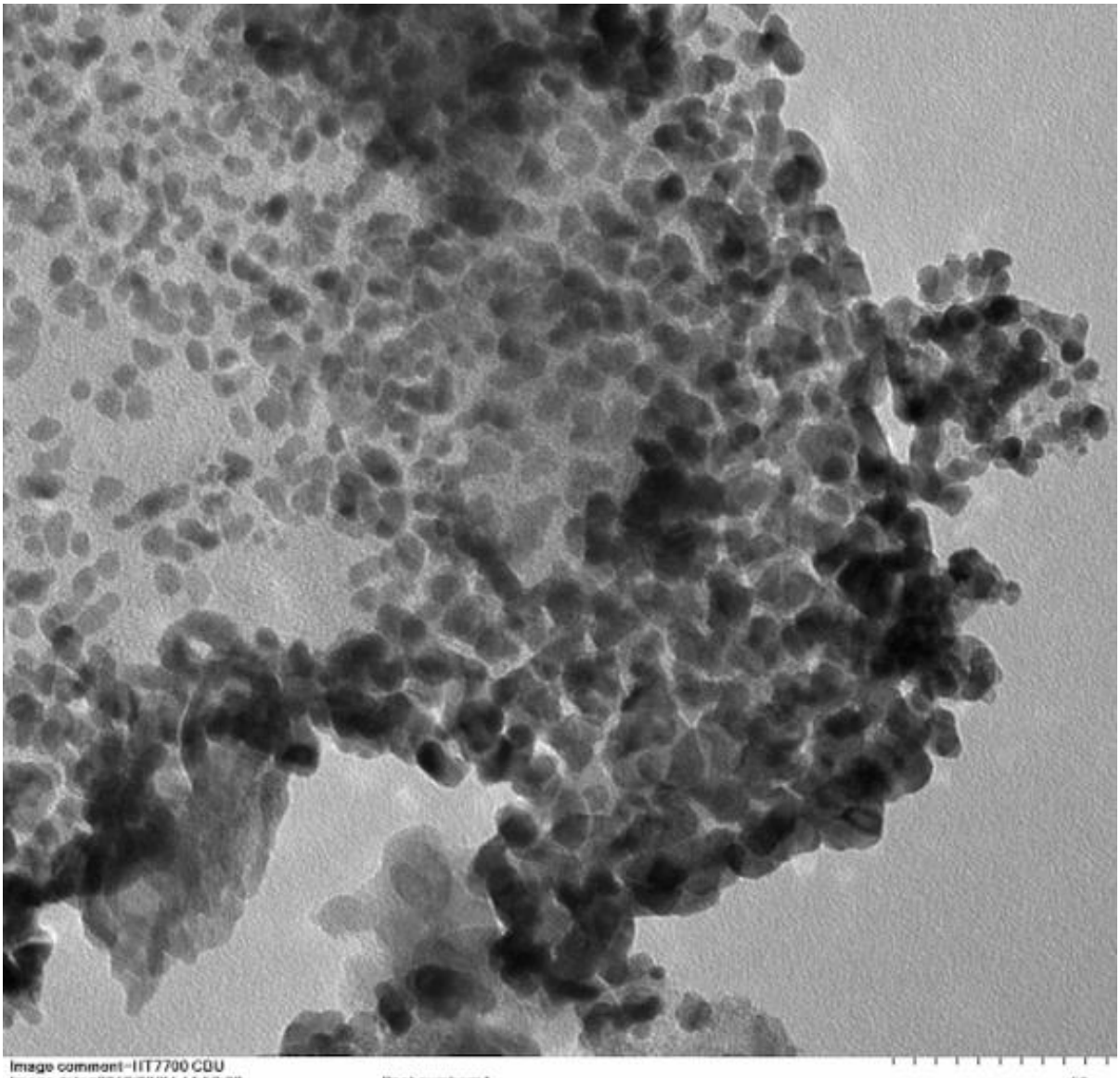
Image comment=HT7700 CDU
Image date=2018/02/21 14:52:39
Image number=0153
Calibration=1.262nm/pixel at x 10.0k
Magnification=x100k
Lens mode=Zoom-1 HC-1
Spot number=4
Image rotation=0°
Acc. voltage=80.0kV
Emission=10.0μA
Stage X=-116 Y=-27 Tilt=-0.1 Azim=0.0
50nm

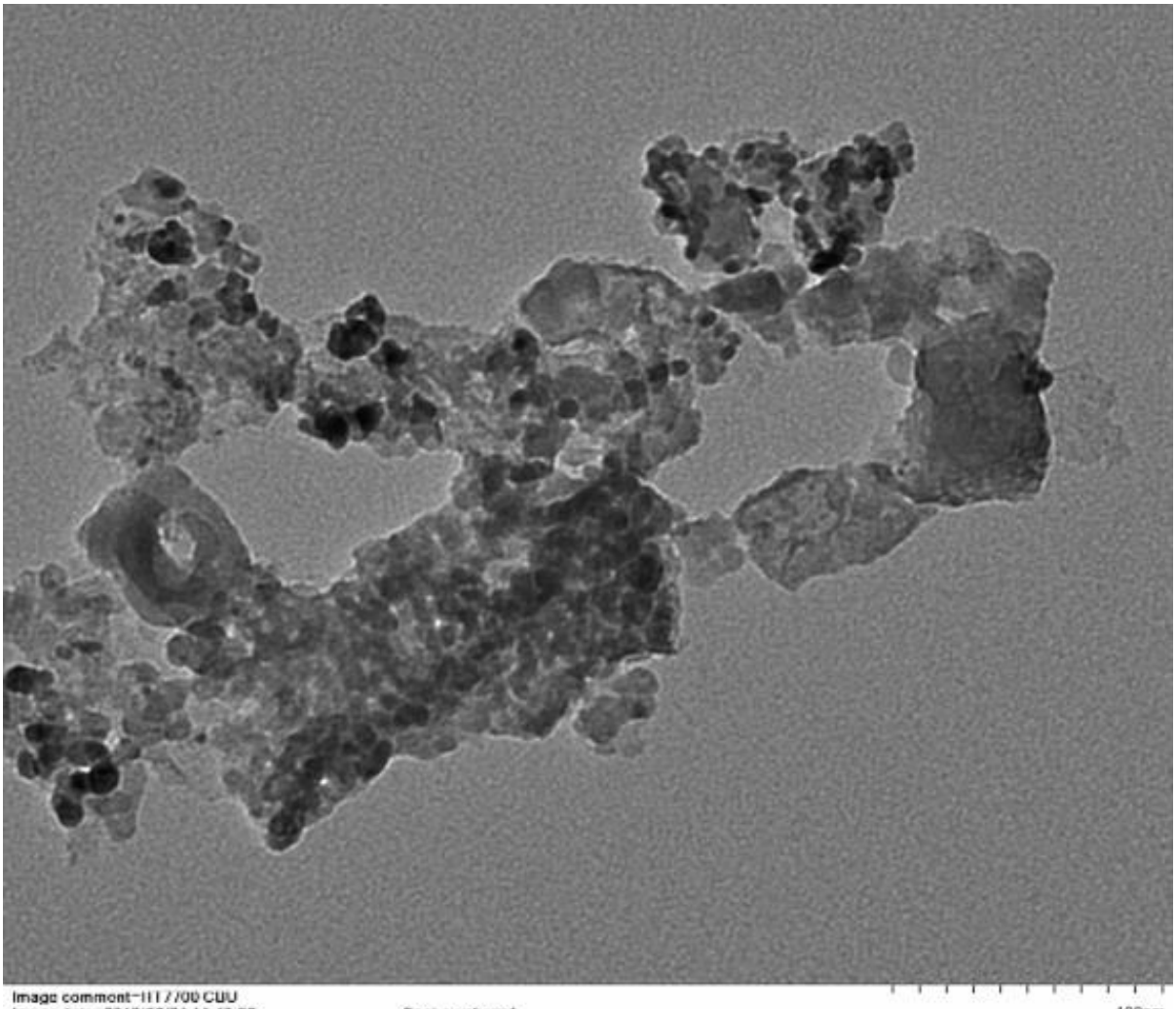
Image comment=HT / 00 CUU
Image date=2018/07/21 14:43:58
Image number=0148
Calibration=1.262nm/pixel at x10.0k
Magnification=x60.0k
Lens mode=Zoom 1 HC 1
Spot number=4
Image rotation=0°
Acc. voltage=80.0kV
Emission=10.0μA
Stage X= 125 Y= 64 Tilt= 0.1 Azim=0.0
100nm

7.1.5 Crab Biochar Catalyst After Use

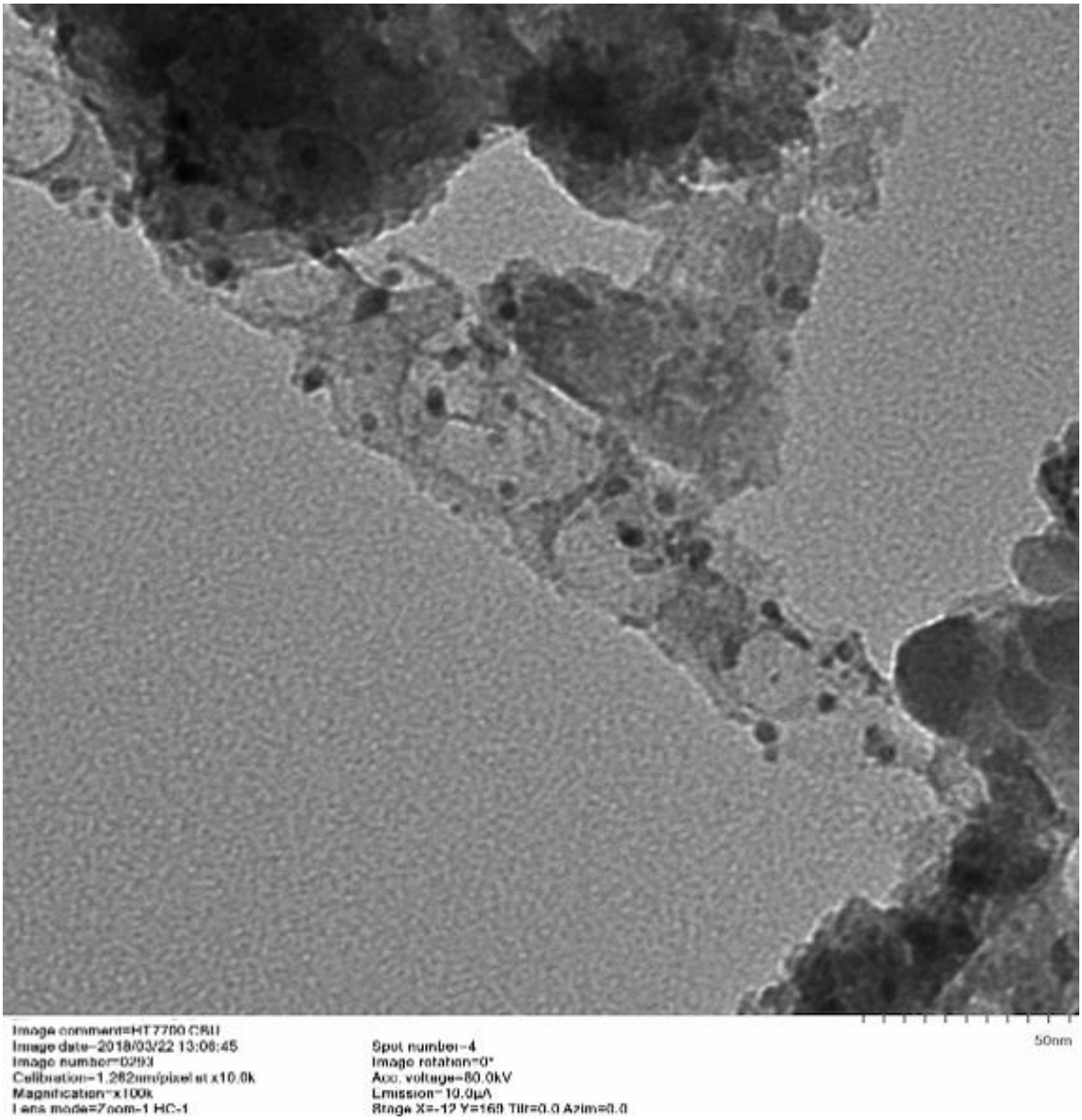

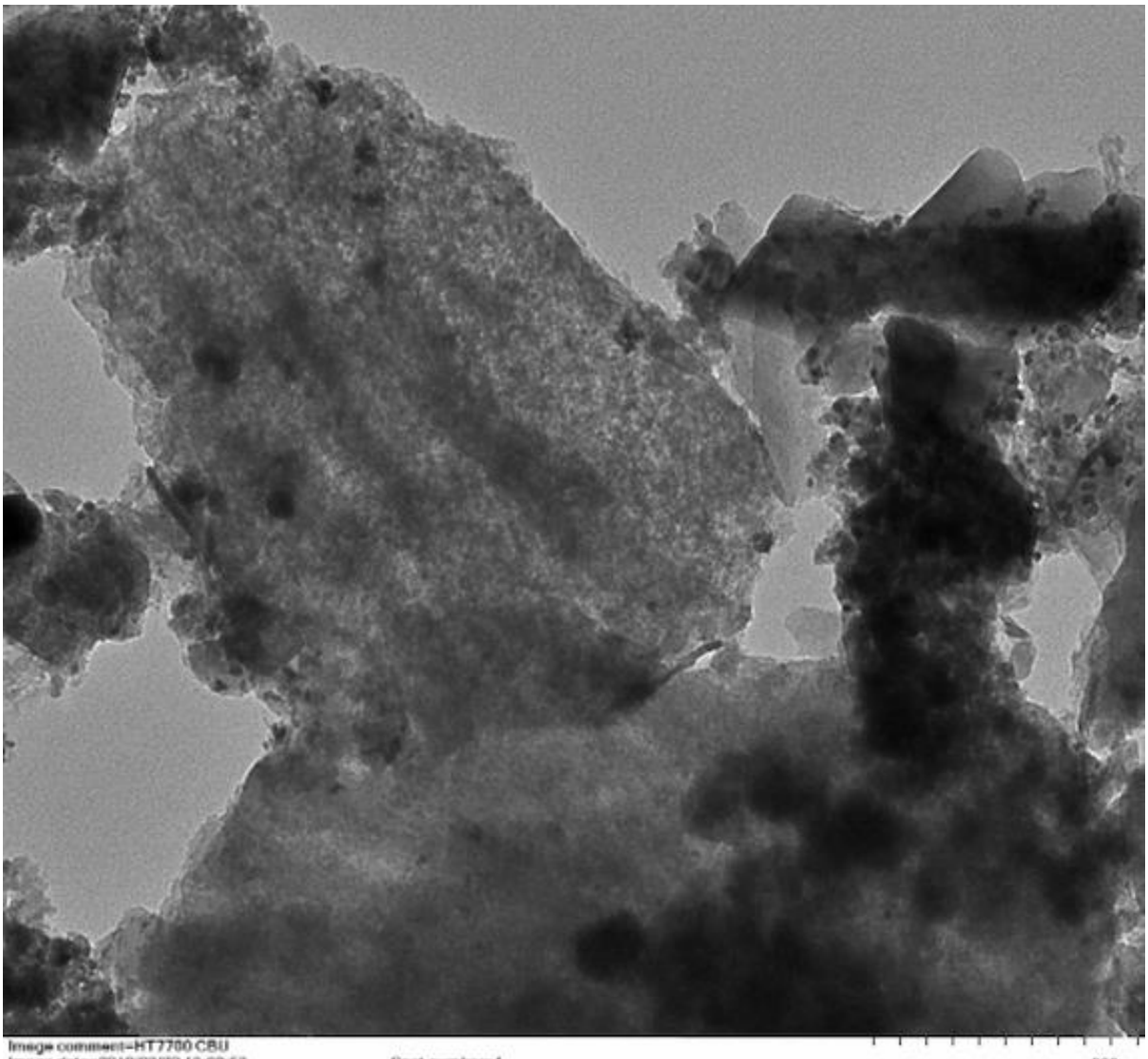
Image comment=HT7700 CBU
Image date=2018/03/22 13:08:53
Image number=0094
Calibration=1.262nm/pixel at x10.0k
Magnification=x30.0k
Lens mode=Zoom-1 HC-1
Spot number=4
Image rotation=0°
Acc. voltage=80.0kV
Emission=10.0μA
Stage X=227 Y=227 Tilt=0.0 Azim=0.0
200nm

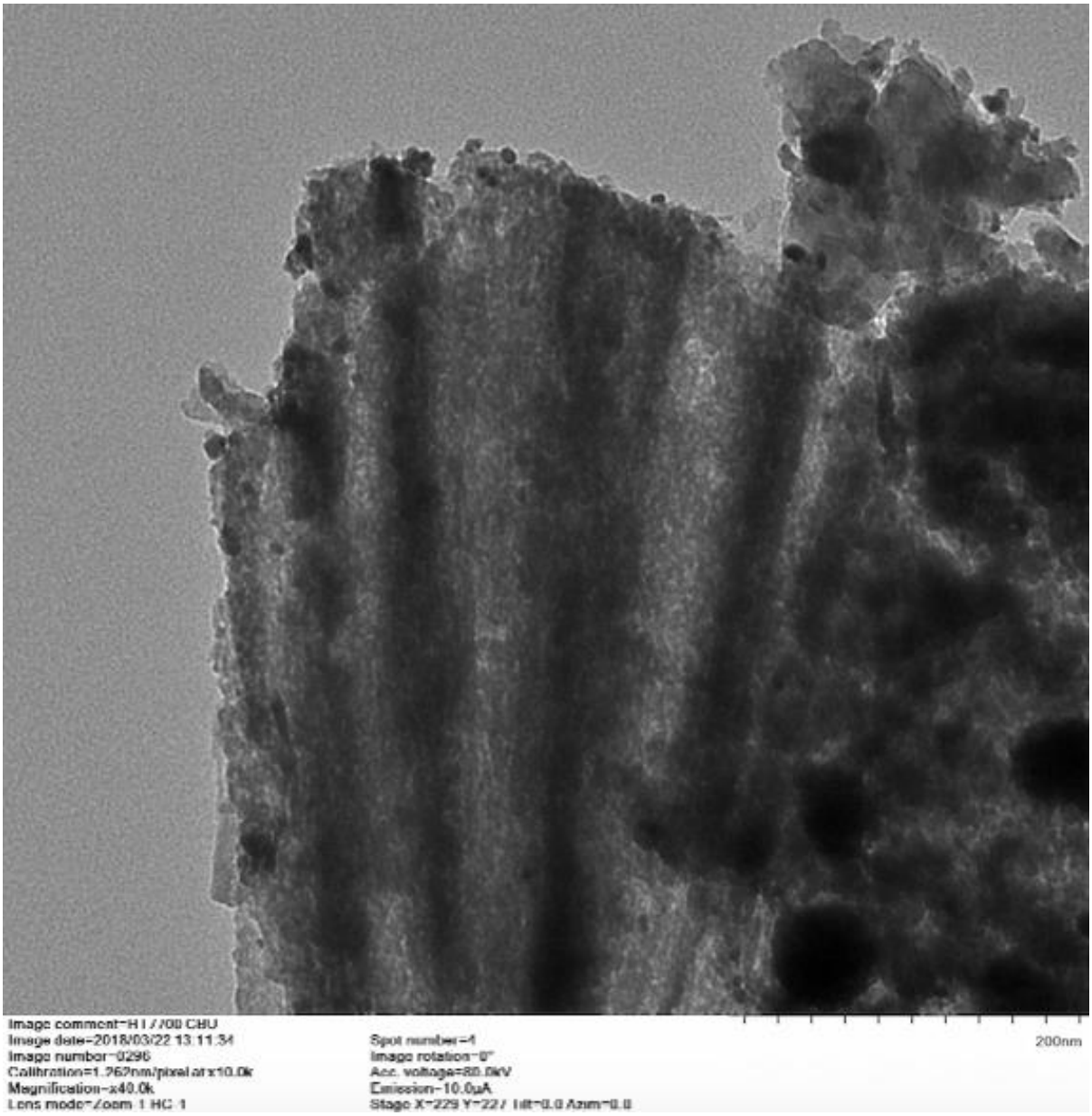
Image comment=H I / 00 CHU
Image date=2018/03/22 13:11:34
Image number=0296
Calibration=1.267nm/pixel at x10.0k
Magnification=x40.0k
Lens mode=Zoom 1 HC 1
Spot number=4
Image rotation=0°
Acc. voltage=80.0kV
Emission=10.0uA
Stage X=229 Y=227 Tilt=0.0 Azim=0.0
200nm